View metadata, citation and similar papers at core.ac.uk

brought to you by CORE

provided by NASA Technical Reports Server

IN-34-CR
7624
P 42

FINITE ELEMENT METHODS OF ANALYSIS FOR 3D INVISCID COMPRESSIBLE FLOWS

NASA Cooperative Agreement NCCW-000010

Final Report for the Period 1 December 1989 : 30 November 1990

Prepared for the

Advanced Aerodynamic Concepts Branch
NASA Ames Research Center
Moffett Field, California 94035, U.S.A.

Submitted by the
Department of Aeronautics
Imperial College of Science, Technology and Medicine
LONDON SW7 2BY
United Kingdom

Principal Investigator : Dr. Jaime Peraire

(NASA-CR-186271) FINITE ELEMENT METHODS OF ANALYSIS FOR 3D INVISCID COMPRESSIBLE FLOWS Final Report, 1 Dec. 1989 - 30 Nov. 1990 (Imperial Coll. of Science and Technology)

N91-21463

Unclas

INTRODUCTION

The applicants have developed a finite element based approach for the solution of 3D compressible flows. The procedure enables flow solutions to be obtained on tetrahedral discretisations of computational domains of complex form. A further development has been the incorporation of a solution adaptive mesh strategy in which the adaptivity is achieved by complete remeshing of the solution domain. During the previous year the applicants have been working with the Advanced Aerodynamics Concepts Branch at NASA Ames Research Center with an implementation of the basic meshing and solution procedure. The objective of the work to be performed over this twelve month period was the transfer of the adaptive mesh technology and also the undertaking of basic research into alternative flow algorithms for the Euler equations on unstructured meshes.

COMPUTER SOFTWARE

J. Peiro visited Ames Research Center during the period 30th April - 4 May, 1990. He undertook the delivery of new versions of the Taylor-Galerkin flow solver (ARCTG), the surface triangulator (ARCST) and the volume generator (ARCVT). In addition he answered queries about the basic algorithms and code organisation and provided information on the modifications present in the updated versions of the code. As a major task under the current grant, the computer code necessary to perform the adaptive remeshing was provided. This code (ARCERR) provides new mesh parameter information based upon an error estimation procedure which uses the second derivatives of the solution. Dr. Erickson of NASA Ames R.C. requested additional codes and we agreed to make these available. These codes provided the ability to generate 3D meshes from a 2D unstructured triangular grid (ARCGB) and for graphic post-processing of the geometry and flow solution (ARCUT). To assist the group at NASA Ames R.C. with the process of familiarisation with the adaptive remeshing codes, J. Peiro undertook in London the adaptive solution of the problem of flow at Mach 1.75

past a 6 degree double wedge aerofoil. This work, which is attached here in the form of Appendix A, was written up in the form of a report and copies provided to Dr. Erickson.

BASIC RESEARCH ON FLOW ALGORITHM DEVELOPMENT

Theory

As a continuation of the work undertaken last year, further investigative work has been undertaken into the possibility of developing a least-squares based Euler solver for implementation on unstructured grids. The current generation of solvers are considered to be far too sensitive to grid quality. The driving force behind these investigations continues to be the hope that a successful implementation will allow for the incorporation of quadratic elements, which should prove to be less sensitive to the quality of the grid being employed.

The formulation which has been tested works with the governing equation

$$\frac{\partial \mathbf{U}}{\partial t} + \frac{\partial \mathbf{F}}{\partial x} + \frac{\partial \mathbf{G}}{\partial y} = \frac{\partial \mathbf{U}}{\partial t} + \mathbf{A}\frac{\partial \mathbf{U}}{\partial x} + \mathbf{B}\frac{\partial \mathbf{U}}{\partial y} = \mathbf{0} \qquad (1)$$

where **A** and **B** are the standard jacobian matrices and **U** is the vector of the conservation variables. This equation is discretised in time by the using a backward difference approximation, which can be written as

$$\frac{\Delta \mathbf{U}}{\Delta t} + \mathbf{A}^n \frac{\partial(\Delta \mathbf{U})}{\partial x} + \mathbf{B}^n \frac{\partial(\Delta \mathbf{U})}{\partial y} = -\left[\frac{\partial \mathbf{F}}{\partial x} + \frac{\partial \mathbf{G}}{\partial y}\right]^n \qquad (2)$$

where $\Delta \mathbf{U} = \mathbf{U}^{n+1} - \mathbf{U}^n$ is the increment in **U** over the timestep Δt and $\mathbf{A}^n = \mathbf{A}(\mathbf{U}^n)$, $\mathbf{B}^n = \mathbf{B}(\mathbf{U}^n)$. The least squares method is based upon the minimisation of the L^2 norm of this equation with respect to $\mathbf{U}^{n+1}$. If the domain is divided into n-noded triangular elements (with n=3 for linear elements and n=6 for quadratic elements), then approximations for $\Delta \mathbf{U}$, $\mathbf{F}^n$ and $\mathbf{G}^n$ can be taken in the form

$$\Delta \mathbf{U} = \Delta \mathbf{U}_i N_i \qquad \mathbf{F}^n = \mathbf{F}_i^n N_i \qquad \mathbf{G}^n = \mathbf{G}_i^n N_i \qquad (3)$$

where N_i denotes the finite element shape function associated with node i of the mesh. A piecewise constant representation is employed for the matrices $\mathbf{A}^n$ and $\mathbf{B}^n$. Upon insertion of these expansions into equation (2), the least squares requirement leads to

$$\mathbf{K}_{ij}\ \Delta \mathbf{U}_j = \mathbf{f}_i \qquad (4)$$

where the entries in the matrix $\mathbf{K}$ and the right hand side vector $\mathbf{f}$ are defined by

$$\mathbf{K}_{ij} = \int_\Omega [\mathbf{I} N_i + \Delta t\, \mathbf{A}^n \frac{\partial N_i}{\partial x} + \Delta t\, \mathbf{B}^n \frac{\partial N_i}{\partial y}]^T [\mathbf{I} N_j + \Delta t\, \mathbf{A}^n \frac{\partial N_j}{\partial x} + \Delta t\, \mathbf{B}^n \frac{\partial N_j}{\partial y}]\, d\Omega$$

$$\mathbf{f}_i = -\int_\Omega [\mathbf{I} N_i + \Delta t\, \mathbf{A}^n \frac{\partial N_j}{\partial x} + \Delta t\, \mathbf{B}^n \frac{\partial N_j}{\partial y}]^T [\frac{\partial \mathbf{F}^n}{\partial x} + \frac{\partial \mathbf{G}^n}{\partial y}]\, d\Omega \qquad (5)$$

When steady state conditions are reached, equation (4) reduces to

$$\int_\Omega \{N_i [\frac{\partial \mathbf{F}^n}{\partial x} + \frac{\partial \mathbf{G}^n}{\partial y}]$$

$$+ \Delta t\, [\mathbf{A}^n \frac{\partial N_i}{\partial x} + \Delta t\, \mathbf{B}^n \frac{\partial N_i}{\partial y}]^T [\mathbf{A}^n \frac{\partial \mathbf{U}^n}{\partial x} + \Delta t\, \mathbf{B}^n \frac{\partial \mathbf{U}^n}{\partial y}]\}\, d\Omega = 0 \qquad (6)$$

and the first term here can be seen to represent a Galerkin form of the steady state Euler equation set, while the second term represents a added diffusion. It can be observed that the amount of added diffusion depends upon the magnitude of the time step and on the jacobian matrices.

The time step employed can be taken to be uniform everywhere or, for the steady computations which are of interest here, lcal timesteps can be employed. It has been found that the convergence rate to steady state is enhanced by the use of local timestepping but that it also leads to the creation of oscillations in the solution in the vicinity of high gradient regions, especially when adaptive mesh refinement is employed. It should also be noted that numerical integration is required for the evaluation of the integrals appearing in equation (5) when curved-sided triangular elements are used in the discretisation of the domain. The solution to equation (4) is achieved by the incomplete Choleski conjugate gradient method.

An Adaptive Refinement Strategy

The diffusion term in equation (6) can be identified with the L^2 norm of the residual and so provides a natural method for indicating where the mesh resolution is insufficient. The standard adaptive remeshing procedure has been modified to use this term as an error indicator.

Numerical Examples

Several examples, involving flows with a supersonic freestream, have been solved with the above algorithm using both linear and quadratic elements. It can be generally seen from the results presented here that quadratic meshes give more accurate results, but they do suffer from slower convergence and tend to exhibit some undesirable oscillations. The flow tangency condition which should be satisfied at solid walls is imposed weakly via a least squares functional term. A characteristic analysis is carried out along the computational boundaries.

(a) Double Wedge Aerofoil. Details of the meshes employed in the solution of this example are shown in figure 1. The free stream Mach number was 2. Also shown in figure 1 are the convergence rates achieved and the distribution of the pressure over the wedge.

(b) 20° Ramp. The free stream Mach number for these computations is 3 and the results are shown in figure 2. The application of the adaptive mesh strategy to this problem is illustrated in figure 3.

(c) Double Compression Corner. The free stream Mach number for this example is 2 and the results obtained are shown in figure 4. The superiority of the quadratic elements over linear elements is most apparent in this example. The solution obtained by adaptive remeshing is shown in figure 5.

(d) Supersonic Flow Past a Cylinder. Supersonic flow at a free stream Mach number of 3 past a circular cylinder is considered in this example. Only one quarter of the cylinder is considered as shown in figure 6. Since the implicit artificial diffusion of the scheme is directly related to the jacobian matrices, it is apparent that problems may be expected in the vicinity of stagnation points. In this case, a small amount of explicit artificial viscosity had to be added to maintain the stability of the scheme. An adapted mesh solution is shown in figure 7.

Current Work

The method developed to date has been shown to be capable of producing encouraging results for compressible flows at low supersonic Mach numbers. However, numerical experiments with quadratic elements have indicated a tendency to produce oscillatory solutions. In addition, when refinement is employed, the method tends to generate oscillations in the vicinity of regions of steep gradient. These problems can be overcome by using a small amount of explicitly added artificial diffusion and this is relatively straightforward in the case of linear elements as several such methods already exist. Extending these methods to produce a diffusion operator on quadratic elements which is consistent with the algorithm is a task which is still to be performed.

CONCLUSIONS

Updated versions of a finite element based set of codes for the solution of the compressible Euler equations on general unstructured meshes have been successfully implemented at NASA Ames R.C. In addition, a facility for obtaining mesh adaptation by complete remeshing has been provided. Work on algorithmic development, with the objective of improving the solution quality on general grids, has proved of limited success and it is apparent that further efforts are needed to improve the situation in this area.

PUBLICATION

J. Peiro, J. Peraire and K. Morgan, 'The computation of 3D aerodynamical flows using unstructured meshes', in *Science and Engineering on Supercomputers*, Edited by Eric J. Pitcher, CML Publications and Springer Verlag, 103-111, 1990.

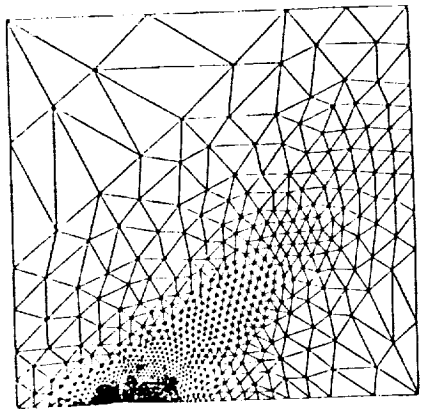

1816 linear elements

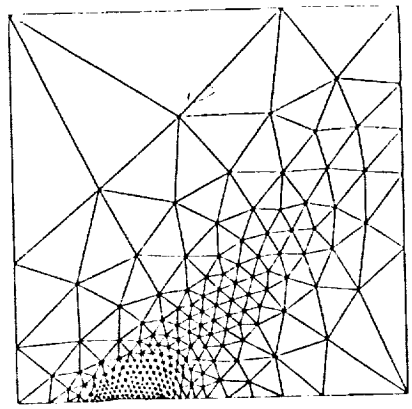

455 quadratic elements

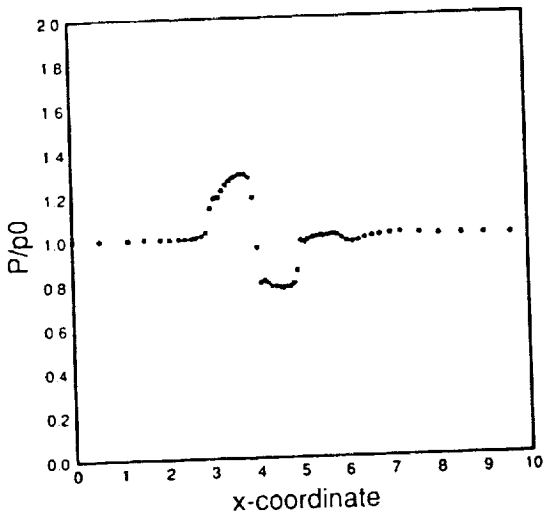

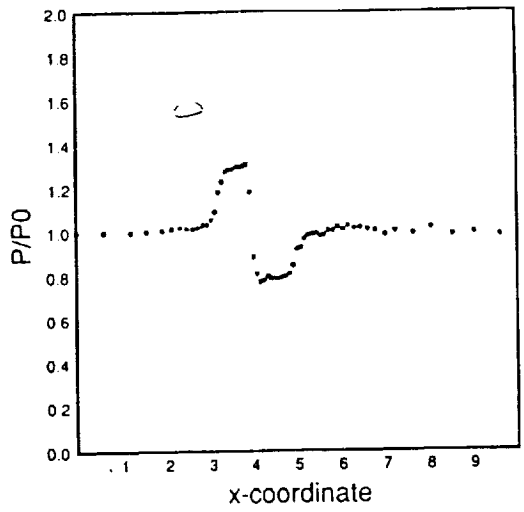

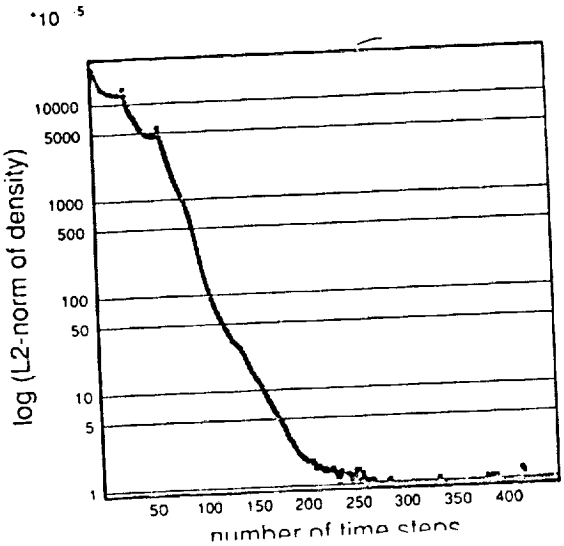

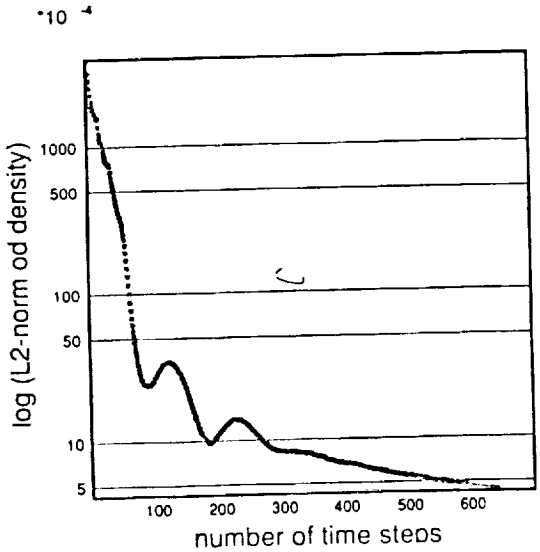

FIGURE 1 Mach 2 flow past a double wedge aerofoil

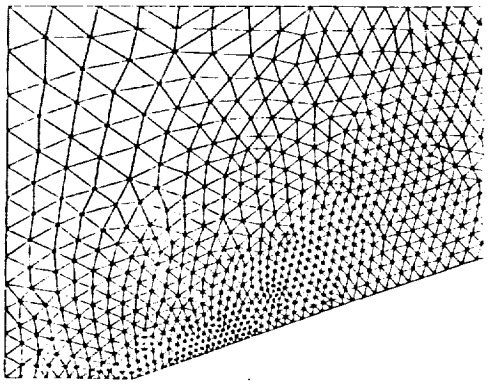

1480 linear elements

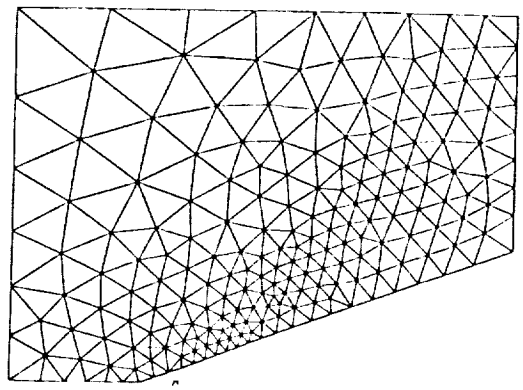

370 quadratic elements

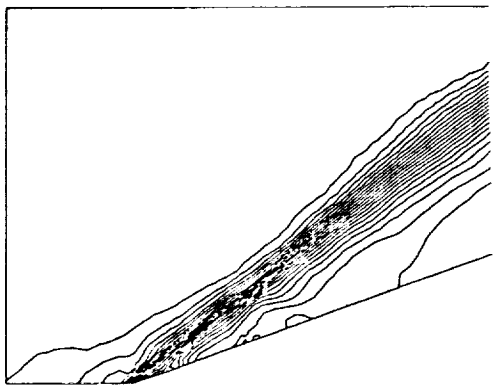

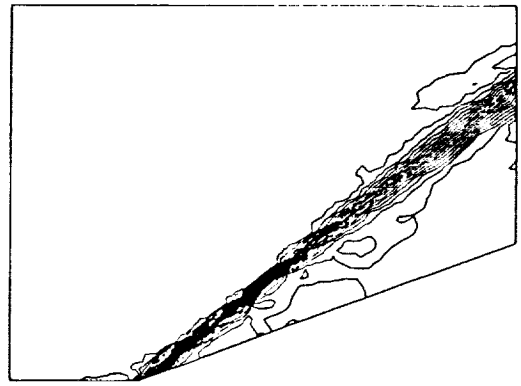

Pressure contours

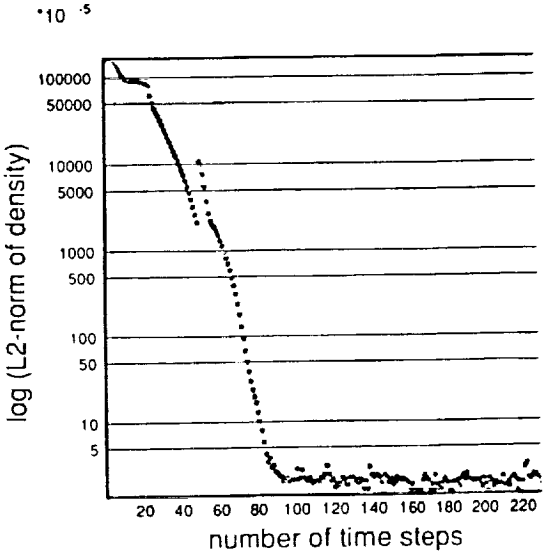

FIGURE 2 Mach 3 flow over a 20° ramp

Pressure contours

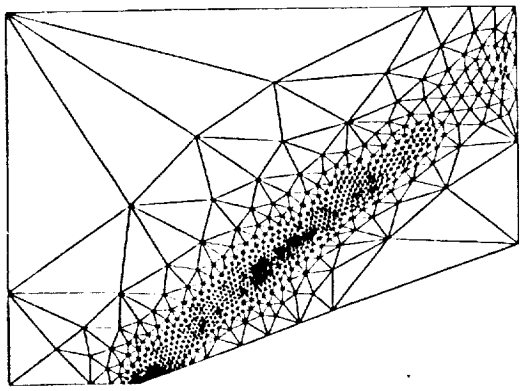

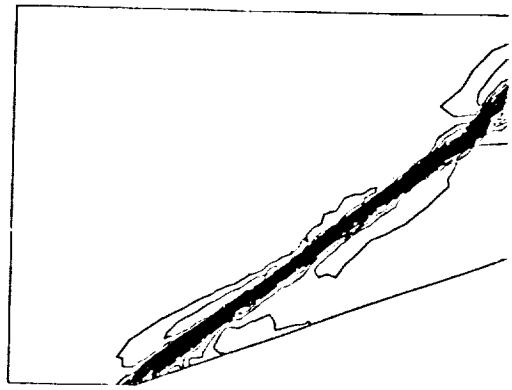

First adaptation 1658 linear elements

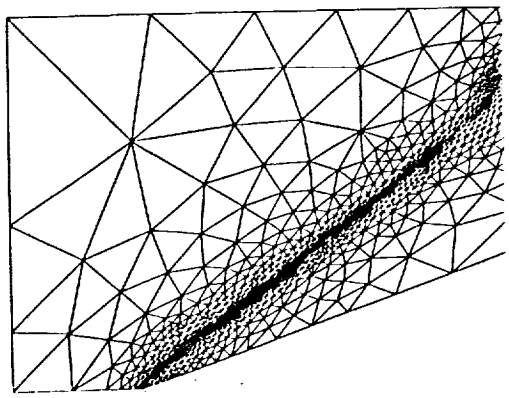

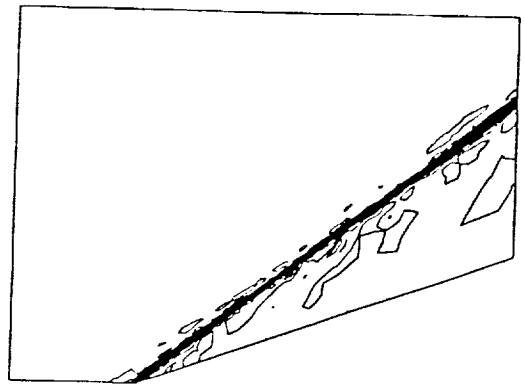

Second adaptation 1092 linear elements

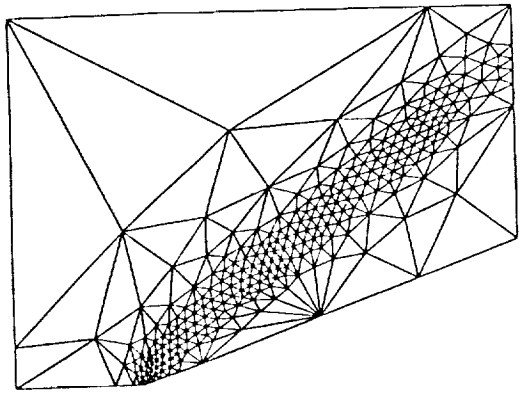

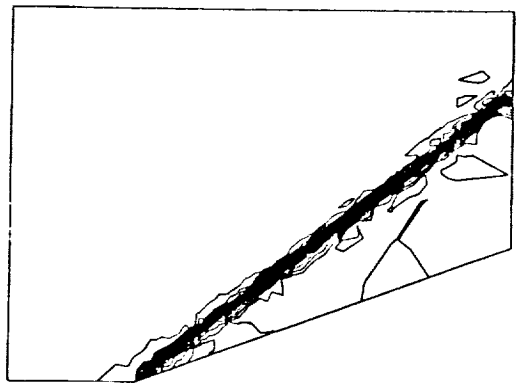

First adaptation 523 quadratic elements

FIGURE 3 Mach 3 flow over a 20° ramp - adapted mesh solutions

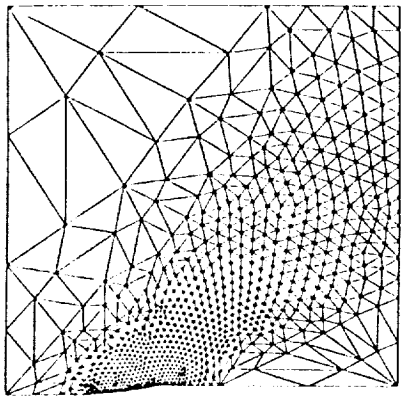

1536 linear elements

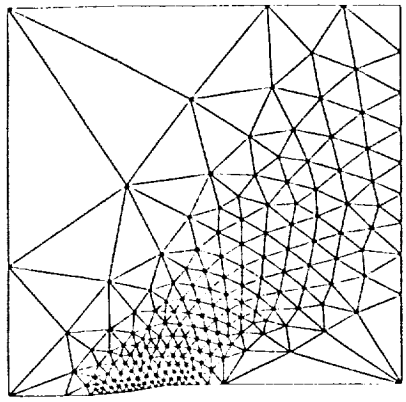

384 quadratic elements

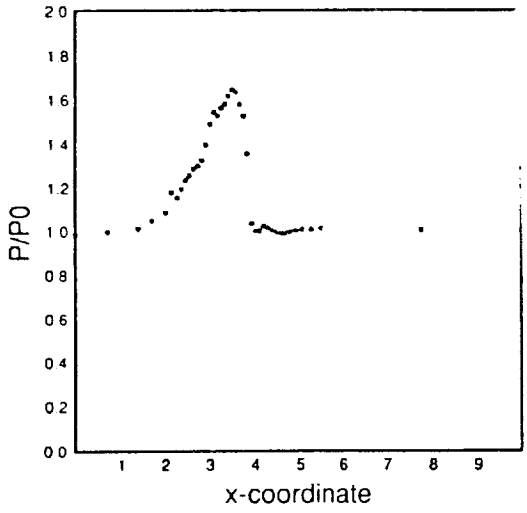

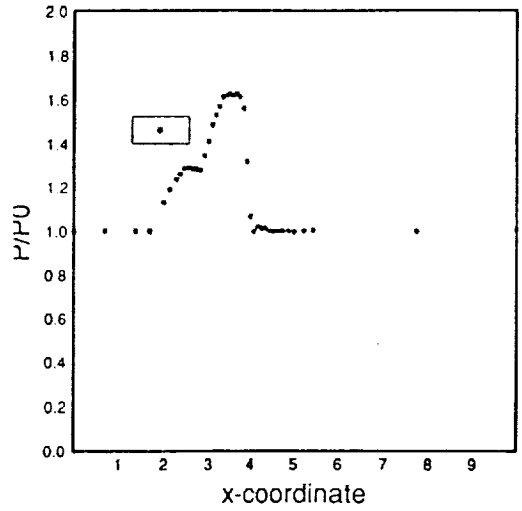

Pressure variation along the surface

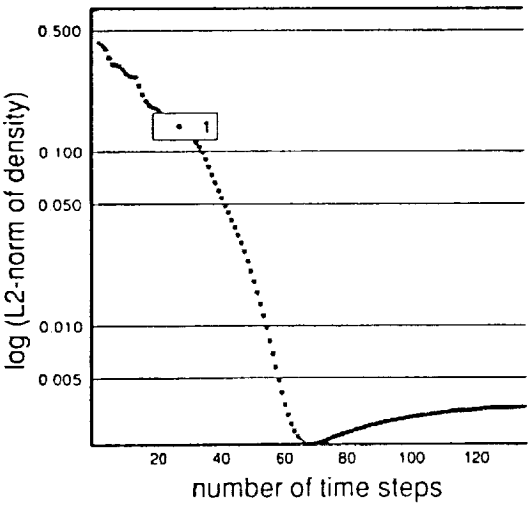

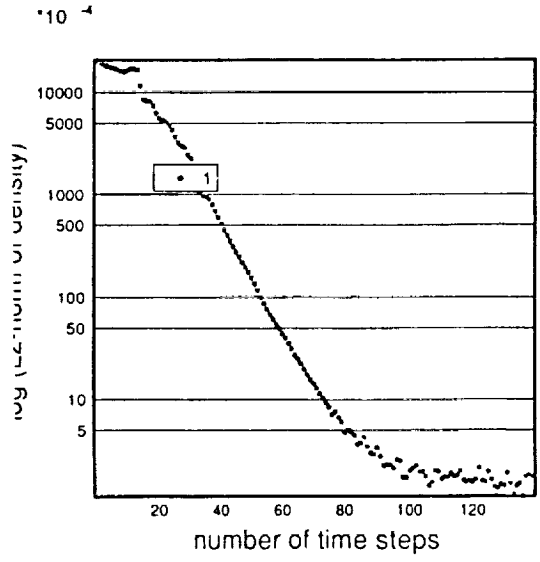

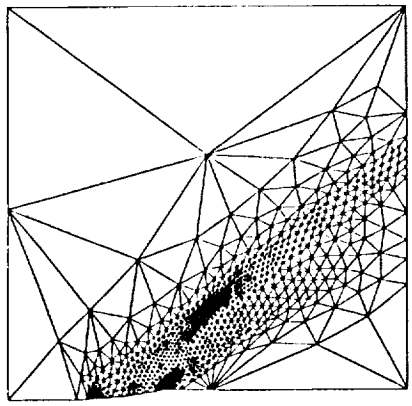

1611 linear elements

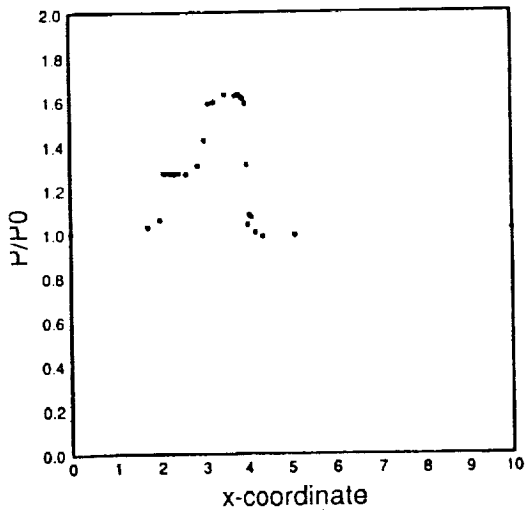

Pressure variation along the surface

FIGURE 5 Mach 2 flow over a double compression corner - adapted mesh solution

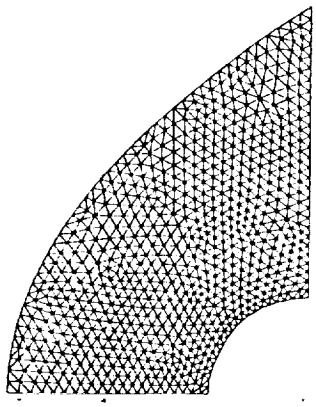

988 linear elements

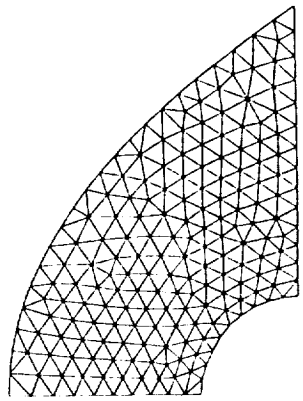

247 quadratic elements

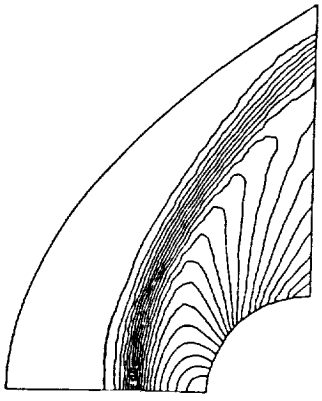

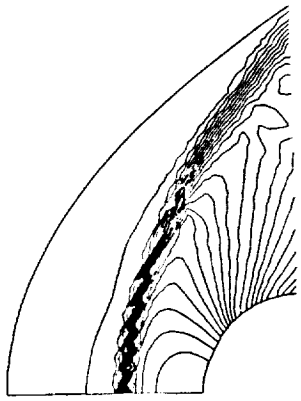

Pressure contours

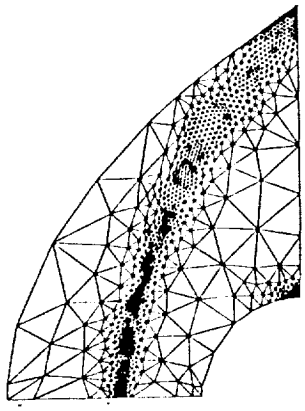

2172 linear elements

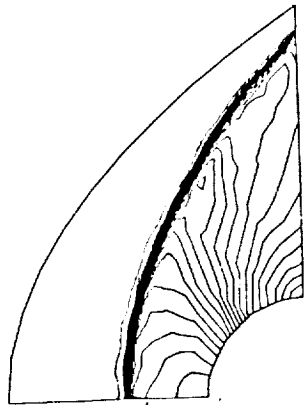

Pressure contours

FIGURE 7 Mach 3 flow over a cylinder - adapted mesh solutions

Report on the solution of the mach 1.75 double wedge

This report presents the results obtained for the solution of the flow past a 6° double wedge at M_∞=1.75 and α=0°. These results have been produced with the same codes currently in use in the Ames Research Center. The source files can be found in the SWANSEA account in RALPH and the names used are:

- **arcst** : Surface triangulator
- **arcvt** : Tetrahedral mesh generator
- **setboun** : Sets the boundary conditions for the 3D mesh
- **arctg** : 3D Taylor-Galerkin Euler solver
- **arcgb** : Generator of initial 3D background meshes from 2D meshes
- **arcerr** : Program for error analysis and definition of background meshes from computed solutions
- **arccut** : Plotting program

The definition of the boundary of the computational domain employed in our computations was provided by Jahed. The data file (dwlp.dat) is enclosed in pages 4-5. A sketch of the computational domain is also included in page 6.

The background grid for the generation of the first mesh has been obtained from a 2D mesh using the program **arcgb**. The input data file (dwlp.bck) and a drawing of the 2D mesh are displayed in pages 7-8. The final background grid data (dwlp.bac) can be found in pages 9-12.

The generated mesh, which will referred to as first mesh, contains 42905 elements, 10180 nodes and 11230 boundary faces. Page 13 shows a view of the surface mesh in the plane y=0.1. A set of preliminary runs was performed on this mesh in order to assess the best choice of parameters for the control file to be used in the code **arctg**. We selected a diffusion coefficient of 1.1 and a smoothing type 2 and tried different types of boundary conditions (parameter istron): weak (0), strong (2) and mixed (1). The computed distributions of the pressure

coefficient on the surface of the wedge at y=0.05 are displayed in page 14.

The solution obtained presents oscillations in both shocks and also in the expansion fan. The use of strong boundary conditions produces the best results giving the smallest oscilations in the trailing edge and the expansion fan. Since all the options produced oscillations on the leading edge shock we opted for the use of a bigger pressure switch coefficient. The control file (dwlp.con) employed for the final run is displayed in page 15. The flow solution obtained after 4000 timesteps starting from free stream values is displayed as follows:

page 16: pressure contours on the plane y=0.1
page 17: mach number contours on the plane y=0.1
page 18: pressure coefficient on the su rface of the wedge at y=0.05 compared with the exact solution
page 19: pressure coefficient at the line z=0.0 y=0.1

Note that the wiggles at the trailing edge and the expansion fan have been substantially reduced. The leading edge oscillations, although smaller, still are present. The magnitude of the oscillations will, however, decrease after the remeshing.

This solution has been utilised to produce a second adapted mesh. The code used is **arcerr** and the "key" variable for the error indication is the mach number. The values employed to produce the background mesh for the generation of the second mesh are:

$\delta_{scaling} = 0.0015$
$\delta_{minimum} = 0.009$
$\delta_{maximum} = 0.2$
stretching = 1.0

The criterion for chosing these values was:

1.- Use a smaller $\delta_{minimum}$ than in the first mesh
2.- Keep the same value $\delta_{maximum}$
3.- Choose $\delta_{scaling}$ such that the number of elements to be generated is aproximately equal or slightly higher than the one used in the first mesh (42905 elements).

The estimated number of elements given by **arcerr** was 52450. The actual number of elements generated by **arcst** and **arcvt** in the second adapted mesh is 69742. The generated surface mesh in the plane y=0.1 is displayed in page 20.

A second Taylor-Galerkin flow solution was computed by using the same parameters as in the first mesh. The control file is included in page 21. The flow solution obtained after 4000 timesteps starting from free stream values is displayed as follows:

page 22: pressure contours on the plane y=0.1
page 23: mach number contours on the plane y=0.1
page 24: pressure coefficient on the su rface of the wedge at y=0.05 compared with the exact solution
page 25: pressure coefficient at the line z=0.0 y=0.1

The new solution presents an overall improvement in definition of the flow features respect to the first solution as it can be observed in pages 26 and 27 which show the comparison between the pressure solutions obtained in the two meshes. Both solutions show a fair agreament with the exact solution.

The convergence curves for the residuals of the derivative of the density for both solutions are displayed in page 28. We have divided the residuals by the second value of the residual (the first one is usually meaningless and it is ignored) to be able to plot both curves together.

The slope of the residuals in the first solution is not steeper than the slope for the second solution as one would have expected. An explanation for this is the fact that the first mesh contains a distorted element that induces a disturbance on the flow solution. This can be clearly noticed on the contours of Mach number in page 17. This does not happen in the second mesh which presents a better convergence curve.

Finally, page 27 contains a drawing of the exact position of point of intersection between the expansion fan and the leading edge shock. At this point the leading edge changes direction and the solution in the neighborhood of the intersection is changed. The "reflected shock" on the boundary is more likely to be a feature of the flow caused by the interaction than a problem of the boundary conditions.

```
s    nsf        ! double wedge loop geometry
1      9
dary edges
2  1 2                              !  LE bd segment
0000   0.10000   0.20040  !w4
0000   0.00000   0.20040  !w1
2  2 3                              ! wedge
0000   0.10000   0.14780  !w5
0000   0.00000   0.14780  !w2
2  1 3                              ! TE
0000   0.10000   0.20040  !w6
0000   0.00000   0.20040  !w3
2  1 8                              ! upper
0000   0.10000   0.20040  !w6
0000   0.10000   0.20040  !w4
2  2 8                               ! front wedge     symm plane 2
0000   0.10000   0.20040  !w4
0000   0.10000   0.14780  !w5
2  3 8                               ! rear wedge
0000   0.10000   0.14780  !w5
0000   0.10000   0.20040  !w6
  2  1  9                           ! upper
0000   0.00000   0.20040  !w3
0000   0.00000   0.20040  !w1
  2  2  9                           ! front wedge symm plane 1
0000   0.00000   0.20040  !w1
0000   0.00000   0.14780  !w2
  2  3  9                           ! rear wedge symm plane 1
0000   0.00000   0.14780  !w2
0000   0.00000   0.20040  !w3
   2  4  5
00000  0.10000   2.00000  !c5
00000  0.00000   2.00000  !c1
   2  5  6
00000  0.10000  -2.00000  !c6
00000  0.00000  -2.00000  !c2
   2  6  7
00000  0.10000  -2.00000  !c7
00000  0.00000  -2.00000  !c3
   2  4  7
00000  0.10000   2.00000  !c8
00000  0.00000   2.00000  !c4
   2  4  8
00000  0.10000   2.00000  !c8
00000  0.10000   2.00000  !c5
   2  5  8
-0000  0.10000   2.00000  !c5
-0000  0.10000  -2.00000  !c6
   2  6  8
-0000  0.10000  -2.00000  !c6
-0000  0.10000  -2.00000  !c7
   2  7  8
-0000  0.10000  -2.00000  !c7
-0000  0.10000   2.00000  !c8
   2  4  9
-0000  0.00000   2.00000  !c4
-0000  0.00000   2.00000  !c1
```

```
19  1  2  5  9
 -2.00000   0.00000   2.00000  !c1
 -2.00000   0.00000  -2.00000  !c2
20  1  2  6  9
 -2.00000   0.00000  -2.00000  !c2
  3.00000   0.00000  -2.00000  !c3
21  1  2  7  9
  3.00000   0.00000  -2.00000  !c3
  3.00000   0.00000   2.00000  !c4
support surfaces
1 1 3 1
 0.00000   0.00000   0.20040  !w1
 1.00000   0.00000   0.20040  !w3
 0.00000   0.10000   0.20040  !w4
2 1 3 1
 0.50000   0.10000   0.14780  !w5
 0.50000   0.00000   0.14780  !w2
 0.00000   0.10000   0.20040  !w4
3 1 3 1
 0.50000   0.00000   0.14780  !w2
 0.50000   0.10000   0.14780  !w5
 1.00000   0.00000   0.20040  !w3
4 1 3 1
 -2.00000   0.00000   2.00000  !c1
 -2.00000   0.10000   2.00000  !c5
  3.00000   0.00000   2.00000  !c4
5 1 3 1
 -2.00000   0.00000  -2.00000  !c2
 -2.00000   0.10000  -2.00000  !c6
 -2.00000   0.00000   2.00000  !c1
6 1 3 1
 -2.00000   0.00000  -2.00000  !c2
  3.00000   0.00000  -2.00000  !c3
 -2.00000   0.10000  -2.00000  !c6
7 1 3 1
  3.00000   0.10000  -2.00000  !c7
  3.00000   0.00000  -2.00000  !c3
  3.00000   0.10000   2.00000  !c8
8 1 3 1
 -2.00000   0.10000  -2.00000  !c6
  3.00000   0.10000  -2.00000  !c7
 -2.00000   0.10000   2.00000  !c5
9 1 3 1
 -2.00000   0.00000  -2.00000  !c2
 -2.00000   0.00000   2.00000  !c1
  3.00000   0.00000  -2.00000  !c3
region definition
1  4
 1 -7 -3  4                          !w1w3w6w4
2  4
 2  -8  -1  5                        !w5w2w1w4
3  4
 -2  6  3  -9                        !w2w5w6w3
4  4
  -10  -14  13  18                   !c1c5c8c4
5  4
  -11    -15  10  19                 !c2c6c5c1c2
```

```
 -12  -16  11                !c2c3c7c6
 21   -13  -17                !c7c3c4c8
  17   14  15  -4  -6  -5     !c6c7c8c5w4w6w5
9 -18  -21  -20  7  8  9     !c2c1c4c3w1w3w2
```

GEOMETRY DEFINITION

21 boundary edges
9 boundary surfaces

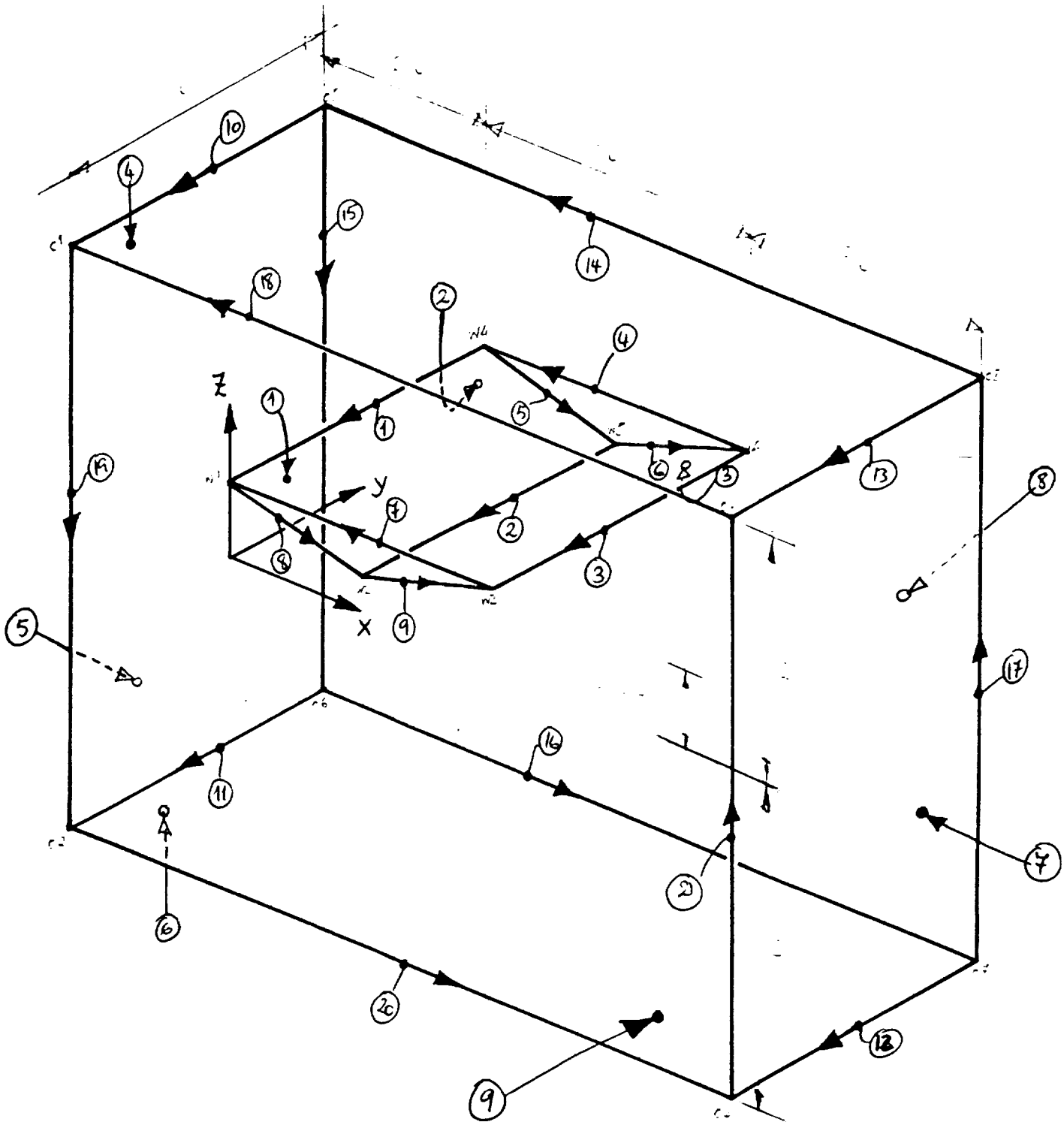

Volume= 2.397

$6 * 4 * 0.1 - 1 * 0.05255$

```
 0.1    0.05    0.
34
 0.00     0.2004     0.02
 0.50     0.1478     0.02
 1.00     0.2004     0.02
 0.50     0.2004     0.06
 0.25     0.1741     0.03
 0.75     0.1741     0.03
-0.25    -0.4000     0.08
 0.20    -0.4000     0.04
 0.50    -0.4000     0.04
 1.00    -0.4000     0.04
 1.50    -0.4000     0.04
 1.50     0.0000     0.04
 1.50     0.4500     0.08
 0.50     0.4500     0.08
-0.25     0.4500     0.08
-0.25     0.0000     0.06
-2.00    -2.0000     0.20
 0.50    -2.0000     0.20
 3.00    -2.0000     0.20
 3.00     0.0000     0.20
 3.00     2.0000     0.20
 0.50     2.0000     0.20
-2.00     2.0000     0.20
-2.00     0.0000     0.20
  1   15   16
  1   16    8
 16    7    8
  1    8    5
  5    8    9
  2    5    9
  2    9    6
  6    9   10
  3    6   10
  3   10   11
  3   11   12
  3   12   13
  3   13   14
  4    3   14
  1    4   14
  1   14   15
 16   15   24
  7   16   24
  7   24   17
  8    7   17
  8   17   18
  9    8   18
 10    9   18
 10   18   19
 11   10   19
 11   19   20
 12   11   20
 12   20   13
 13   20   21
 13   21   22
 14   13   22
 32   15   14   22
 33   15   22   23
 34   15   23   24
```

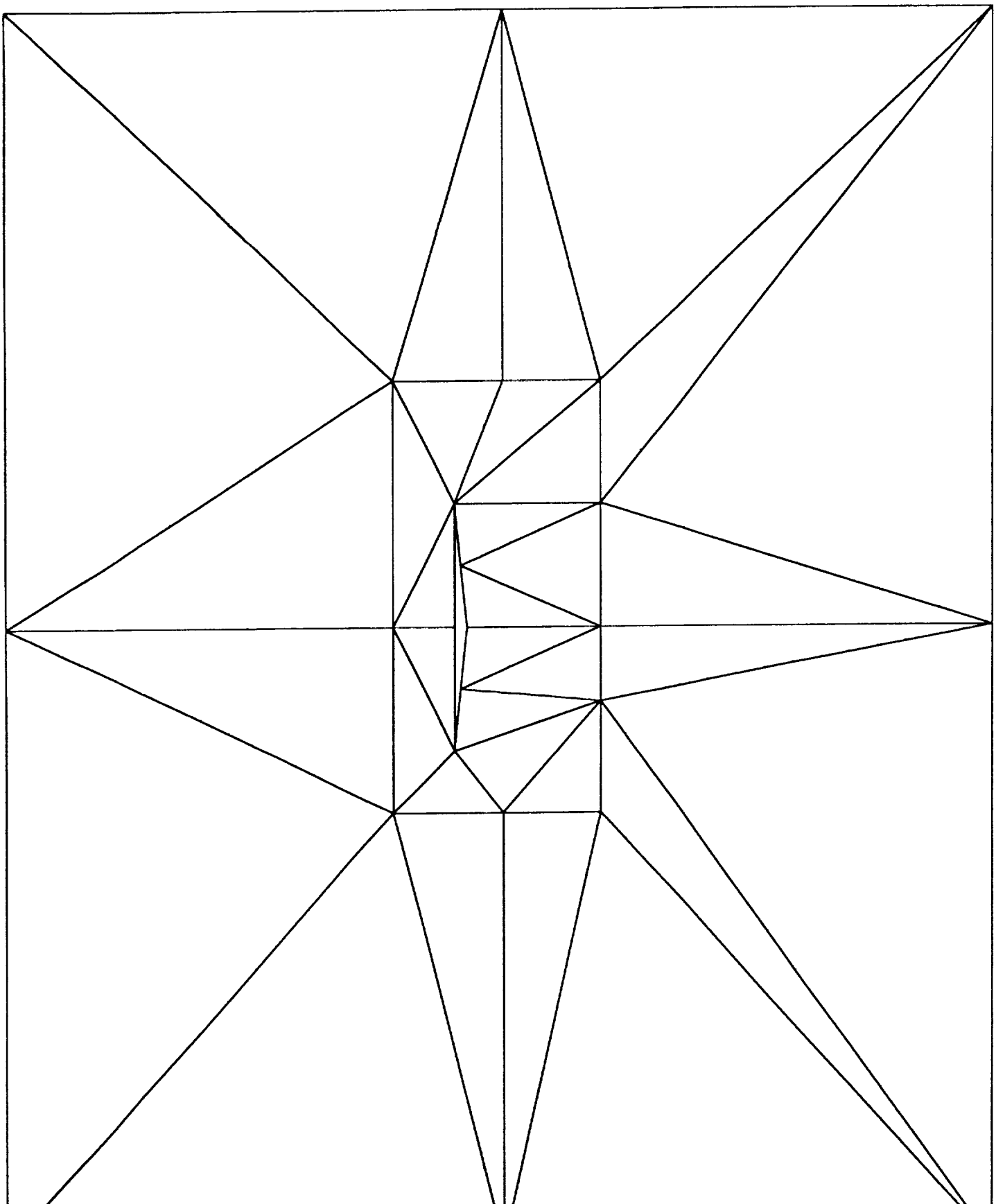

```
t b.g.
  204
        .0000        .1000        .2004
0 .000  .000  .020  .000 1.000  .000   .020  .000  .000 1.000   .020
        .5000        .1000        .1478
0 .000  .000  .020  .000 1.000  .000   .020  .000  .000 1.000   .020
       1.0000        .1000        .2004
0 .000  .000  .020  .000 1.000  .000   .020  .000  .000 1.000   .020
        .5000        .1000        .2004
0 .000  .000  .060  .000 1.000  .000   .060  .000  .000 1.000   .060
        .2500        .1000        .1741
0 .000  .000  .030  .000 1.000  .000   .030  .000  .000 1.000   .030
        .7500        .1000        .1741
0 .000  .000  .030  .000 1.000  .000   .030  .000  .000 1.000   .030
       -.2500        .1000       -.4000
0 .000  .000  .080  .000 1.000  .000   .080  .000  .000 1.000   .080
        .2000        .1000       -.4000
0 .000  .000  .040  .000 1.000  .000   .040  .000  .000 1.000   .040
        .5000        .1000       -.4000
0 .000  .000  .040  .000 1.000  .000   .040  .000  .000 1.000   .040
       1.0000        .1000       -.4000
0 .000  .000  .040  .000 1.000  .000   .040  .000  .000 1.000   .040
       1.5000        .1000       -.4000
0 .000  .000  .040  .000 1.000  .000   .040  .000  .000 1.000   .040
       1.5000        .1000        .0000
0 .000  .000  .040  .000 1.000  .000   .040  .000  .000 1.000   .040
       1.5000        .1000        .4500
0 .000  .000  .080  .000 1.000  .000   .080  .000  .000 1.000   .080
        .5000        .1000        .4500
0 .000  .000  .080  .000 1.000  .000   .080  .000  .000 1.000   .080
       -.2500        .1000        .4500
0 .000  .000  .080  .000 1.000  .000   .080  .000  .000 1.000   .080
       -.2500        .1000        .0000
0 .000  .000  .060  .000 1.000  .000   .060  .000  .000 1.000   .060
      -2.0000        .1000      -2.0000
0 .000  .000  .200  .000 1.000  .000   .200  .000  .000 1.000   .200
        .5000        .1000      -2.0000
0 .000  .000  .200  .000 1.000  .000   .200  .000  .000 1.000   .200
       3.0000        .1000      -2.0000
0 .000  .000  .200  .000 1.000  .000   .200  .000  .000 1.000   .200
       3.0000        .1000        .0000
0 .000  .000  .200  .000 1.000  .000   .200  .000  .000 1.000   .200
       3.0000        .1000       2.0000
0 .000  .000  .200  .000 1.000  .000   .200  .000  .000 1.000   .200
        .5000        .1000       2.0000
0 .000  .000  .200  .000 1.000  .000   .200  .000  .000 1.000   .200
      -2.0000        .1000       2.0000
0 .000  .000  .200  .000 1.000  .000   .200  .000  .000 1.000   .200
      -2.0000        .1000        .0000
0 .000  .000  .200  .000 1.000  .000   .200  .000  .000 1.000   .200
        .0000        .0500        .2004
0 .000  .000  .020  .000 1.000  .000   .020  .000  .000 1.000   .020
        .5000        .0500        .1478
0 .000  .000  .020  .000 1.000  .000   .020  .000  .000 1.000   .020
       1.0000        .0500        .2004
0 .000  .000  .020  .000 1.000  .000   .020  .000  .000 1.000   .020
        .5000        .0500        .2004
```

```
1.000  .000  .000  .060  .000 1.000  .000   .060  .000  .000 1.000   .060
  29        .2500        .0500        .1741
1.000  .000  .000  .030  .000 1.000  .000   .030  .000  .000 1.000   .030
  30        .7500        .0500        .1741
1.000  .000  .000  .030  .000 1.000  .000   .030  .000  .000 1.000   .030
  31       -.2500        .0500       -.4000
1.000  .000  .000  .080  .000 1.000  .000   .080  .000  .000 1.000   .080
  32        .2000        .0500       -.4000
1.000  .000  .000  .040  .000 1.000  .000   .040  .000  .000 1.000   .040
  33        .5000        .0500       -.4000
1.000  .000  .000  .040  .000 1.000  .000   .040  .000  .000 1.000   .040
  34       1.0000        .0500       -.4000
1.000  .000  .000  .040  .000 1.000  .000   .040  .000  .000 1.000   .040
  35       1.5000        .0500       -.4000
1.000  .000  .000  .040  .000 1.000  .000   .040  .000  .000 1.000   .040
  36       1.5000        .0500        .0000
1.000  .000  .000  .040  .000 1.000  .000   .040  .000  .000 1.000   .040
  37       1.5000        .0500        .4500
1.000  .000  .000  .080  .000 1.000  .000   .080  .000  .000 1.000   .080
  38        .5000        .0500        .4500
1.000  .000  .000  .080  .000 1.000  .000   .080  .000  .000 1.000   .080
  39       -.2500        .0500        .4500
1.000  .000  .000  .080  .000 1.000  .000   .080  .000  .000 1.000   .080
  40       -.2500        .0500        .0000
1.000  .000  .000  .060  .000 1.000  .000   .060  .000  .000 1.000   .060
  41      -2.0000        .0500      -2.0000
1.000  .000  .000  .200  .000 1.000  .000   .200  .000  .000 1.000   .200
  42        .5000        .0500      -2.0000
1.000  .000  .000  .200  .000 1.000  .000   .200  .000  .000 1.000   .200
  43       3.0000        .0500      -2.0000
1.000  .000  .000  .200  .000 1.000  .000   .200  .000  .000 1.000   .200
  44       3.0000        .0500        .0000
1.000  .000  .000  .200  .000 1.000  .000   .200  .000  .000 1.000   .200
  45       3.0000        .0500       2.0000
1.000  .000  .000  .200  .000 1.000  .000   .200  .000  .000 1.000   .200
  46        .5000        .0500       2.0000
1.000  .000  .000  .200  .000 1.000  .000   .200  .000  .000 1.000   .200
  47      -2.0000        .0500       2.0000
1.000  .000  .000  .200  .000 1.000  .000   .200  .000  .000 1.000   .200
  48      -2.0000        .0500        .0000
1.000  .000  .000  .200  .000 1.000  .000   .200  .000  .000 1.000   .200
  49        .0000        .0000        .2004
1.000  .000  .000  .020  .000 1.000  .000   .020  .000  .000 1.000   .020
  50        .5000        .0000        .1478
1.000  .000  .000  .020  .000 1.000  .000   .020  .000  .000 1.000   .020
  51       1.0000        .0000        .2004
1.000  .000  .000  .020  .000 1.000  .000   .020  .000  .000 1.000   .020
  52        .5000        .0000        .2004
1.000  .000  .000  .060  .000 1.000  .000   .060  .000  .000 1.000   .060
  53        .2500        .0000        .1741
1.000  .000  .000  .030  .000 1.000  .000   .030  .000  .000 1.000   .030
  54        .7500        .0000        .1741
1.000  .000  .000  .030  .000 1.000  .000   .030  .000  .000 1.000   .030
  55       -.2500        .0000       -.4000
1.000  .000  .000  .080  .000 1.000  .000   .080  .000  .000 1.000   .080
  56        .2000        .0000       -.4000
1.000  .000  .000  .040  .000 1.000  .000   .040  .000  .000 1.000   .040
```

9

```
        .5000        .0000       -.4000
0  .000  .000   .040  .000 1.000  .000   .040  .000  .000 1.000   .040
      1.0000        .0000       -.4000
0  .000  .000   .040  .000 1.000  .000   .040  .000  .000 1.000   .040
      1.5000        .0000       -.4000
0  .000  .000   .040  .000 1.000  .000   .040  .000  .000 1.000   .040
      1.5000        .0000        .0000
0  .000  .000   .040  .000 1.000  .000   .040  .000  .000 1.000   .040
      1.5000        .0000        .4500
0  .000  .000   .080  .000 1.000  .000   .080  .000  .000 1.000   .080
      .5000        .0000        .4500
0  .000  .000   .080  .000 1.000  .000   .080  .000  .000 1.000   .080
     -.2500        .0000        .4500
0  .000  .000   .080  .000 1.000  .000   .080  .000  .000 1.000   .080
     -.2500        .0000        .0000
0  .000  .000   .060  .000 1.000  .000   .060  .000  .000 1.000   .060
    -2.0000        .0000       -2.0000
0  .000  .000   .200  .000 1.000  .000   .200  .000  .000 1.000   .200
      .5000        .0000       -2.0000
0  .000  .000   .200  .000 1.000  .000   .200  .000  .000 1.000   .200
     3.0000        .0000       -2.0000
0  .000  .000   .200  .000 1.000  .000   .200  .000  .000 1.000   .200
     3.0000        .0000        .0000
0  .000  .000   .200  .000 1.000  .000   .200  .000  .000 1.000   .200
     3.0000        .0000       2.0000
0  .000  .000   .200  .000 1.000  .000   .200  .000  .000 1.000   .200
      .5000        .0000       2.0000
0  .000  .000   .200  .000 1.000  .000   .200  .000  .000 1.000   .200
    -2.0000        .0000       2.0000
0  .000  .000   .200  .000 1.000  .000   .200  .000  .000 1.000   .200
    -2.0000        .0000        .0000
0  .000  .000   .200  .000 1.000  .000   .200  .000  .000 1.000   .200
    1   15   16   40
   15   39   40   25
    1   15   40   25
    1   16    8   32
   16   40   32   25
    1   16   32   25
   16    7    8   32
    7   31   32   40
   16    7   32   40
    1    8    5   29
    8   32   29   25
    1    8   29   25
    5    8    9   33
    8   32   33   29
    5    8   33   29
    2    5    9   33
    5   29   33   26
    2    5   33   26
    2    9    6   30
    9   33   30   26
    2    9   30   26
    6    9   10   34
    9   33   34   30
    6    9   34   30
    3    6   10   34
```

```
26    6   30   34   27
27    3    6   34   27
28    3   10   11   35
29   10   34   35   27
30    3   10   35   27
31    3   11   12   36
32   11   35   36   27
33    3   11   36   27
34    3   12   13   37
35   12   36   37   27
36    3   12   37   27
37    3   13   14   38
38   13   37   38   27
39    3   13   38   27
40    4    3   14   38
41    3   27   38   28
42    4    3   38   28
43    1    4   14   38
44    4   28   38   25
45    1    4   38   25
46    1   14   15   39
47   14   38   39   25
48    1   14   39   25
49   16   15   24   48
50   15   39   48   40
51   16   15   48   40
52    7   16   24   48
53   16   40   48   31
54    7   16   48   31
55    7   24   17   41
56   24   48   41   31
57    7   24   41   31
58    8    7   17   41
59    7   31   41   32
60    8    7   41   32
61    8   17   18   42
62   17   41   42   32
63    8   17   42   32
64    9    8   18   42
65    8   32   42   33
66    9    8   42   33
67   10    9   18   42
68    9   33   42   34
69   10    9   42   34
70   10   18   19   43
71   18   42   43   34
72   10   18   43   34
73   11   10   19   43
74   10   34   43   35
75   11   10   43   35
76   11   19   20   44
77   19   43   44   35
78   11   19   44   35
79   12   11   20   44
80   11   35   44   36
81   12   11   44   36
82   12   20   13   37
```

	20	44	37	36
	12	20	37	36
	13	20	21	45
5	20	44	45	37
7	13	20	45	37
1	13	21	22	46
9	21	45	46	37
0	13	21	46	37
	14	13	22	46
2	13	37	46	38
4	14	13	46	38
3	15	14	22	46
6	14	38	46	39
5	15	14	46	39
7	15	22	23	47
8	22	46	47	39
9	15	22	47	39
0	15	23	24	48
1	23	47	48	39
2	15	23	48	39
3	25	39	40	64
4	39	63	64	49
5	25	39	64	49
6	25	40	32	56
7	40	64	56	49
8	25	40	56	49
9	40	31	32	56
0	31	55	56	64
1	40	31	56	64
2	25	32	29	53
3	32	56	53	49
4	25	32	53	49
5	29	32	33	57
6	32	56	57	53
7	29	32	57	53
8	26	29	33	57
9	29	53	57	50
0	26	29	57	50
1	26	33	30	54
2	33	57	54	50
3	26	33	54	50
4	30	33	34	58
5	33	57	58	54
6	30	33	58	54
7	27	30	34	58
8	30	54	58	51
9	27	30	58	51
0	27	34	35	59
1	34	58	59	51
2	27	34	59	51
3	27	35	36	60
4	35	59	60	51
5	27	35	60	51
6	27	36	37	61
7	36	60	61	51
8	27	36	61	51
9	27	37	38	62

140	37	61	62	51
141	27	37	62	51
142	28	27	38	62
143	27	51	62	52
144	28	27	62	52
145	25	28	38	62
146	28	52	62	49
147	25	28	62	49
148	25	38	39	63
149	38	62	63	49
150	25	38	63	49
151	40	39	48	72
152	39	63	72	64
153	40	39	72	64
154	31	40	48	72
155	40	64	72	55
156	31	40	72	55
157	31	48	41	65
158	48	72	65	55
159	31	48	65	55
160	32	31	41	65
161	31	55	65	56
162	32	31	65	56
163	32	41	42	66
164	41	65	66	56
165	32	41	66	56
166	33	32	42	66
167	32	56	66	57
168	33	32	66	57
169	34	33	42	66
170	33	57	66	58
171	34	33	66	58
172	34	42	43	67
173	42	66	67	58
174	34	42	67	58
175	35	34	43	67
176	34	58	67	59
177	35	34	67	59
178	35	43	44	68
179	43	67	68	59
180	35	43	68	59
181	36	35	44	68
182	35	59	68	60
183	36	35	68	60
184	36	44	37	61
185	44	68	61	60
186	36	44	61	60
187	37	44	45	69
188	44	68	69	61
189	37	44	69	61
190	37	45	46	70
191	45	69	70	61
192	37	45	70	61
193	38	37	46	70
194	37	61	70	62
195	38	37	70	62
196	39	38	46	70

7	38	62	70	63
8	39	38	70	63
9	39	46	47	71
0	46	70	71	63
1	39	46	71	63
2	39	47	48	72
3	47	71	72	63
4	39	47	72	63

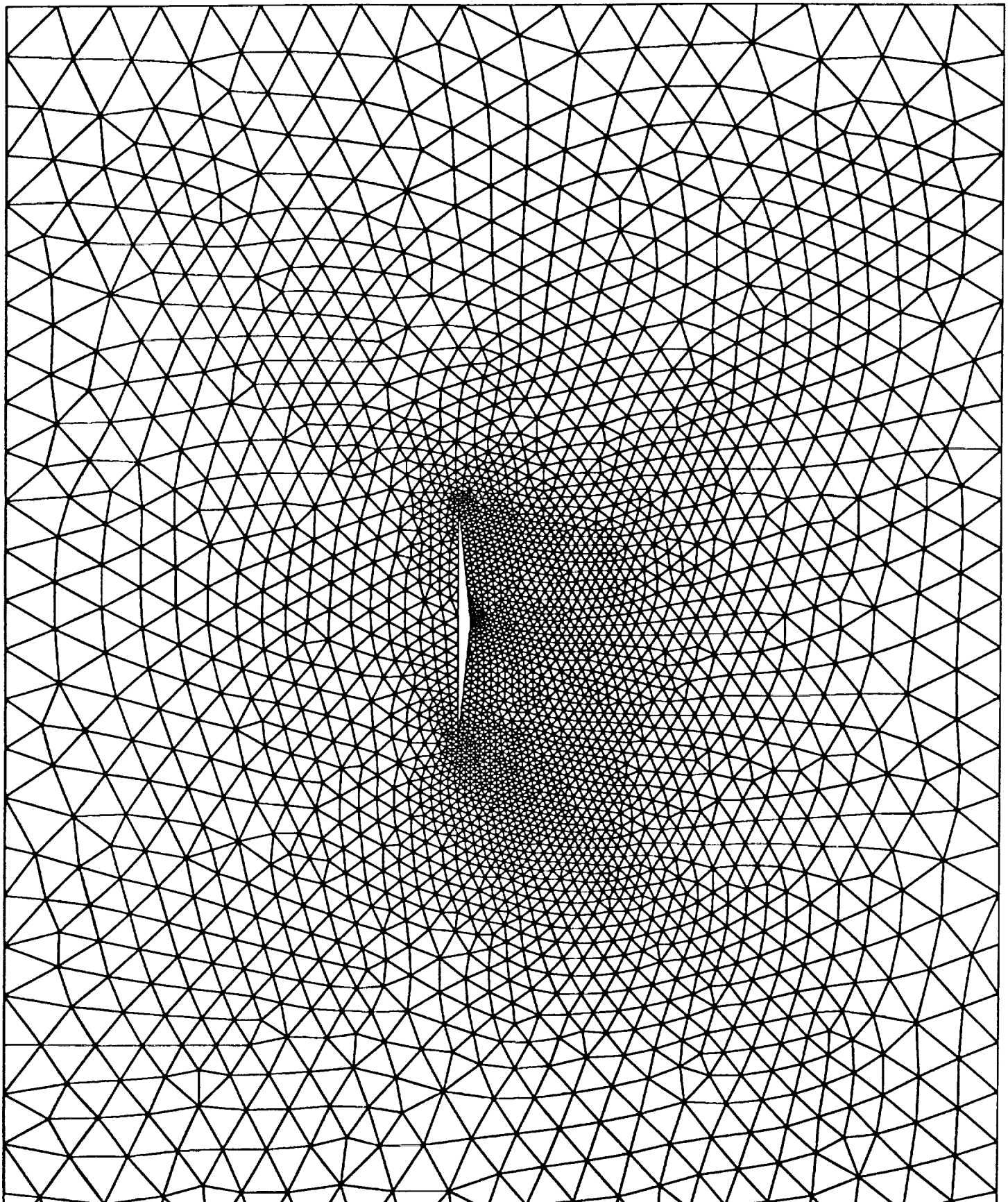

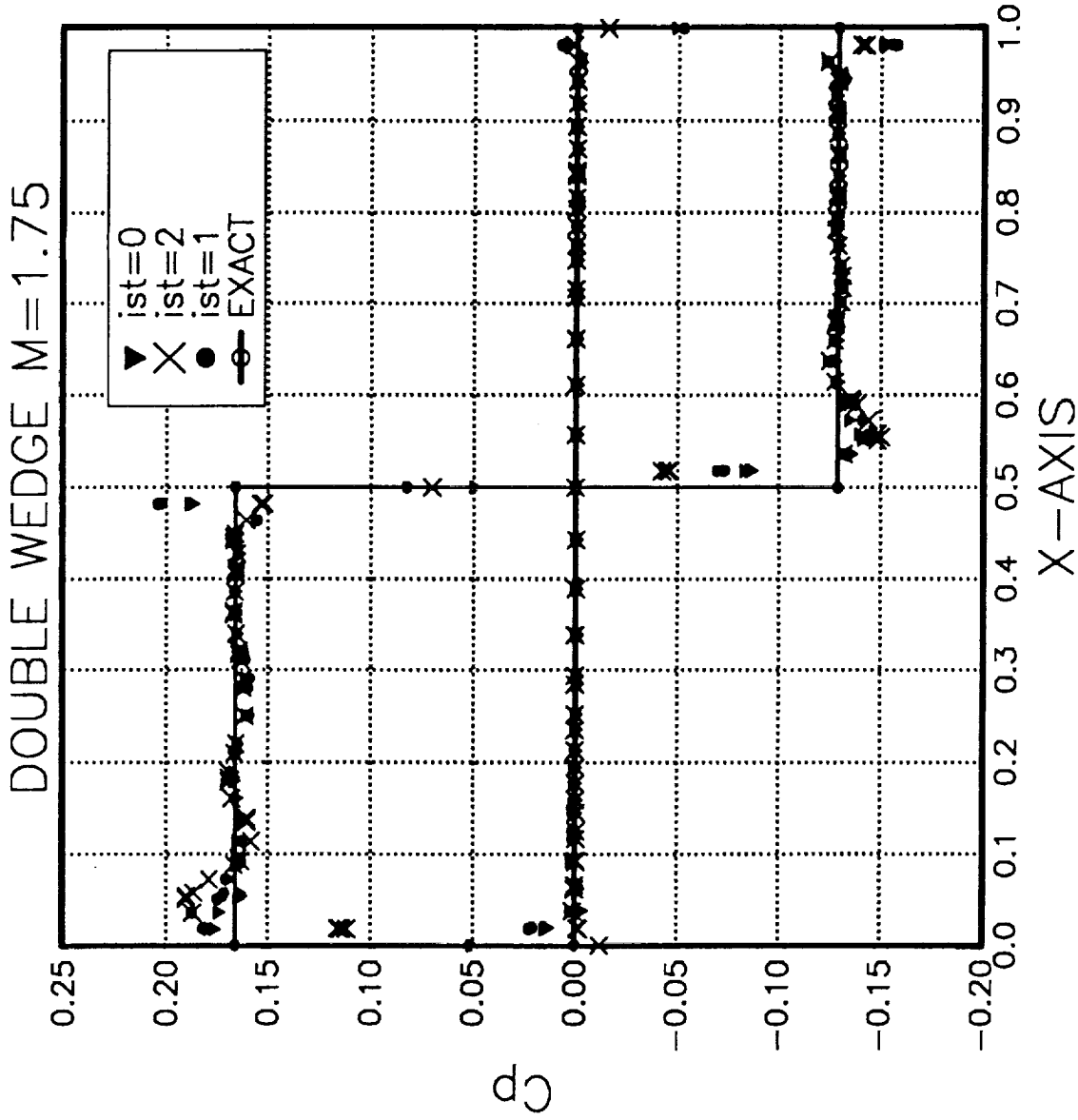
DOUBLE WEDGE M=1.75
ist=0
ist=2
ist=1
EXACT
Cp
X-AXIS
0.25
0.20
0.15
0.10
0.05
0.00
-0.05
-0.10
-0.15
-0.20
0.0
0.1
0.2
0.3
0.4
0.5
0.6
0.7
0.8
0.9
1.0

```
*********************************************
  double wedge  M=1.75, a=0 -> first mesh  ***
*********************************************
mber of dimensions

ements  points  boundary faces
2905    10180    11230
mma  pres.sw.coef. smoothing type  epsilon ivisc     wbr
.4     5.0           2             0.       0     1.
 of far field b.c.

inf   uxinf     uyinf       uzinf       pinf       machinf
.      1.        0.0         0.0       0.2332361     1.75
 of engine b.c.

ime  niter  ilots(0=GLOBAL)
000     1       1
fety f. ifct nquan ido   max clima
7       0   2   1 3      0.8
rmat:  g.input  u. input u.output niout
         -1       -2        1     0
moo nsmoo
   0.25   2
talpy damping coefficent
.0
idual  out  log  lift  out  log   axis    chord
        1    1          1    1    0. 0. 1.  1.
f iterations between smoothing
  1
ron  icheck
2      0
tial time and iter. n.
.0   0
put file name  (DN= )
p
p.geo

of cpu
```

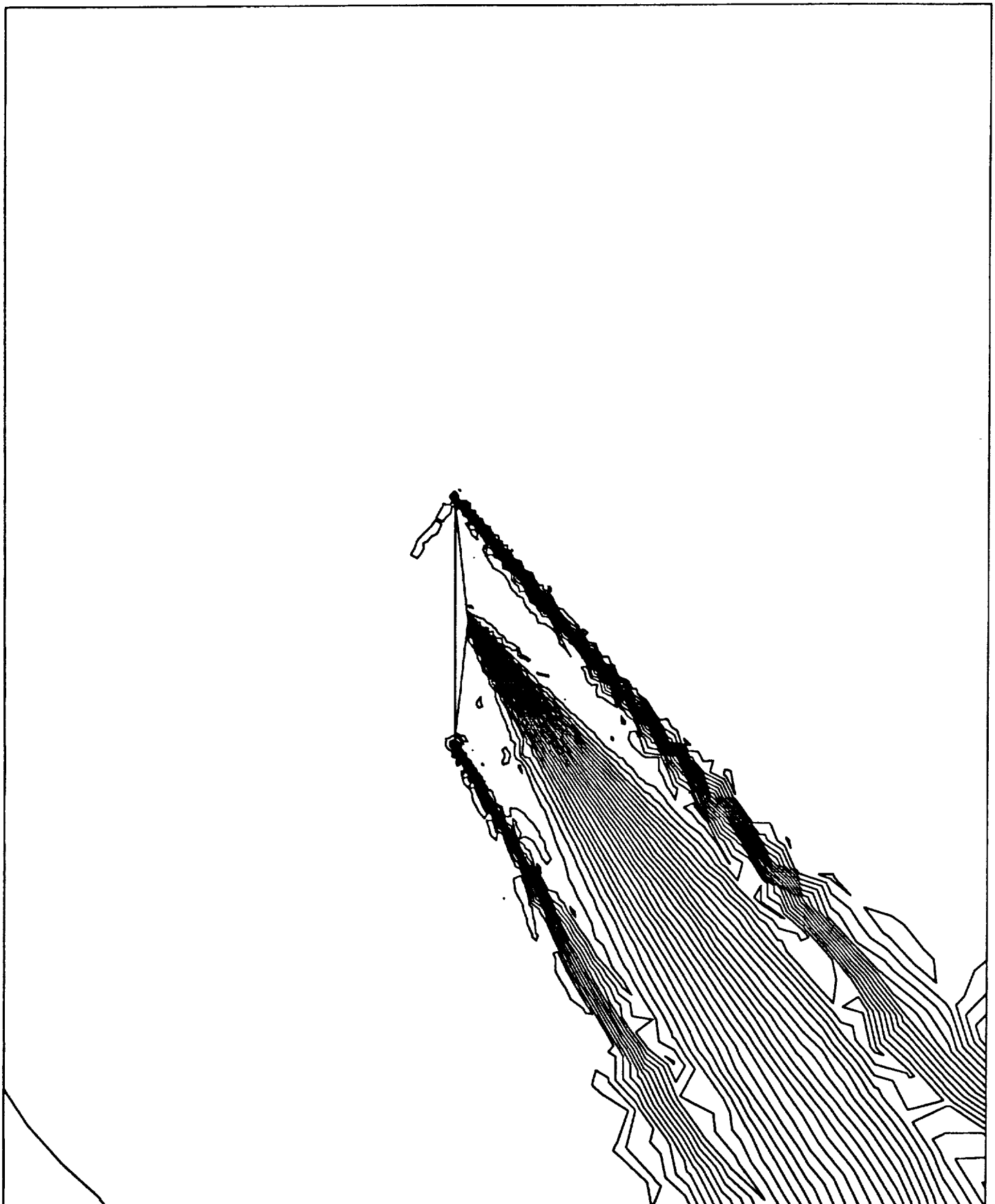

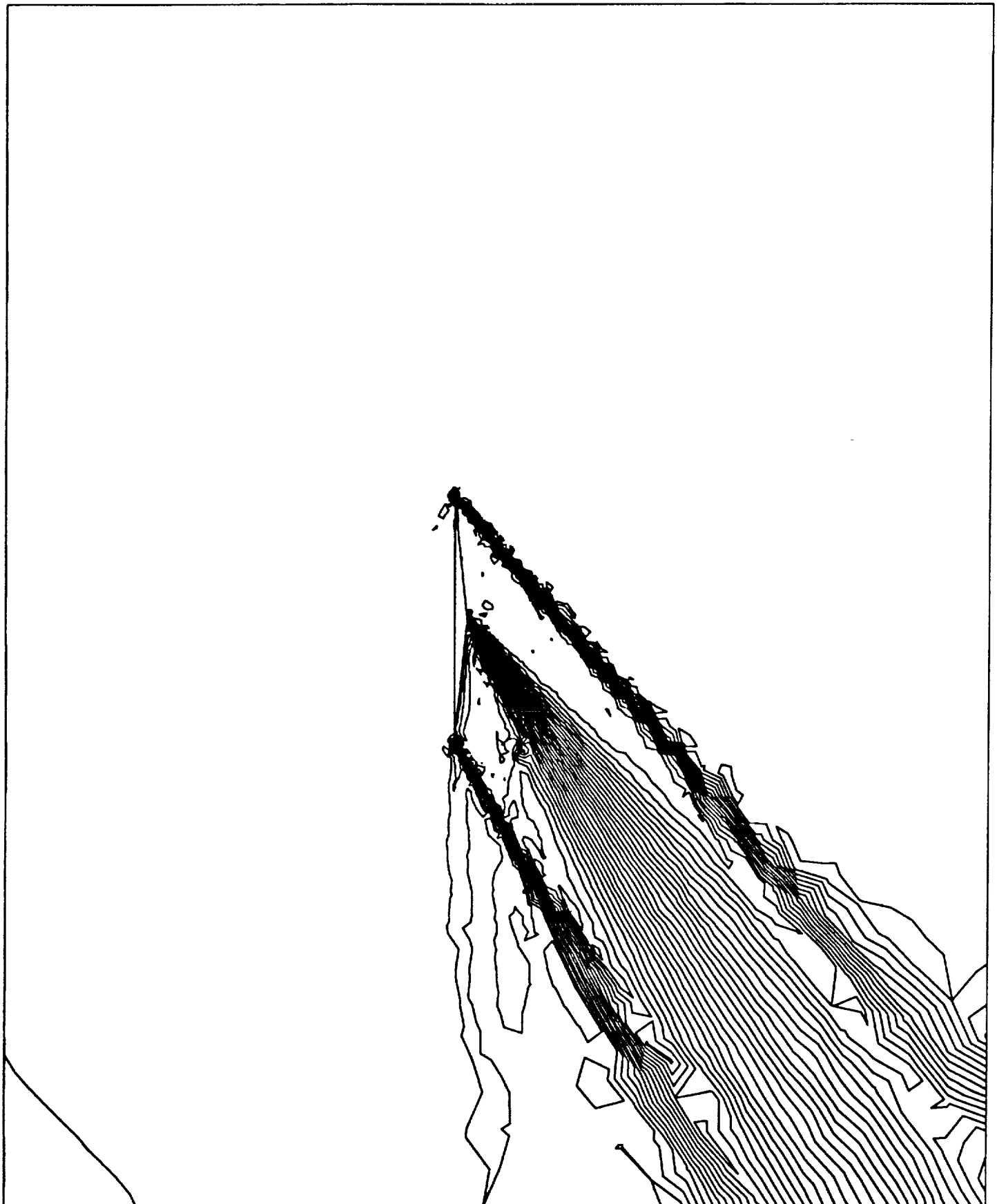

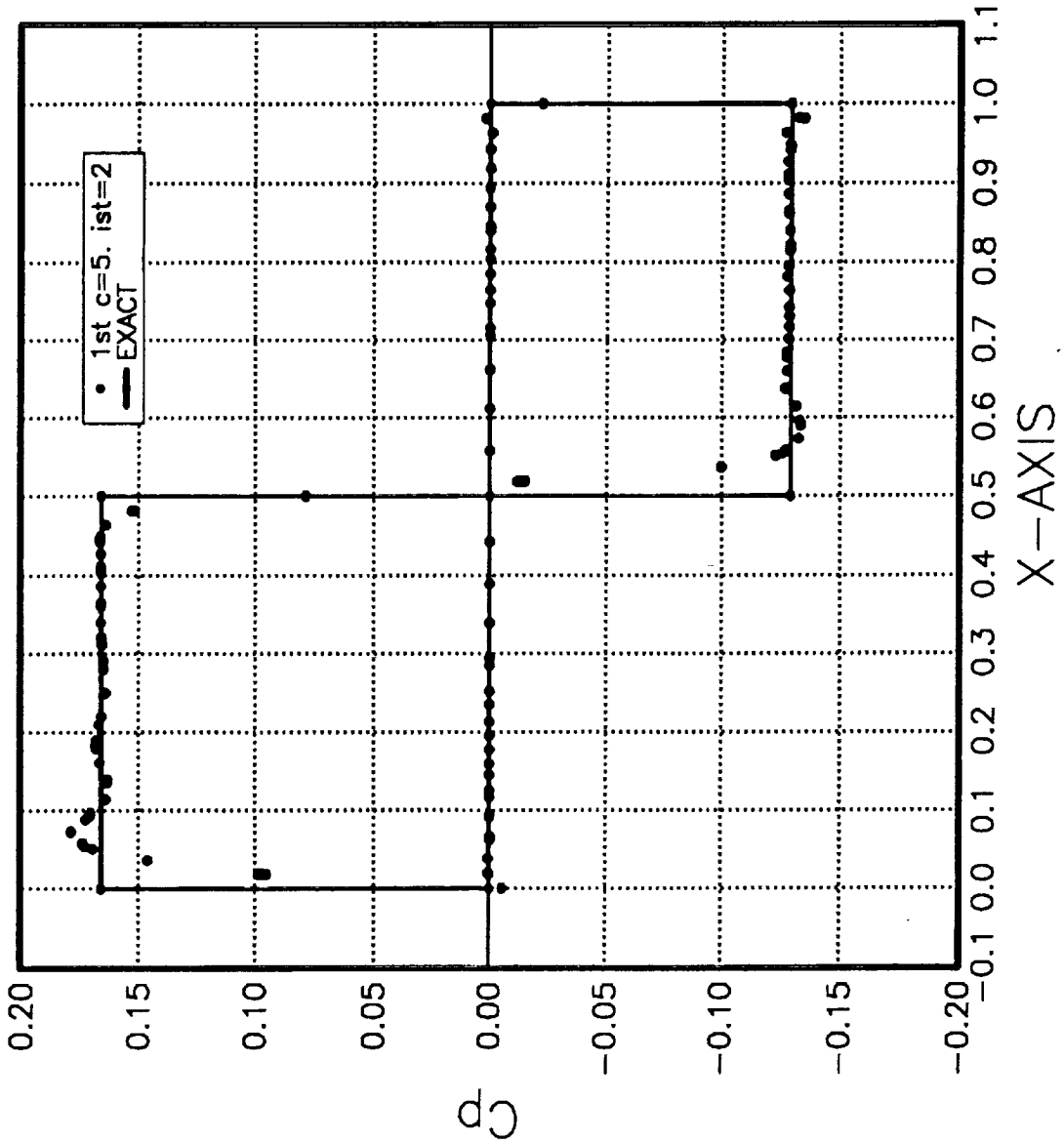
1st c=5. ist=2
EXACT
0.20
0.15
0.10
0.05
0.00
−0.05
−0.10
−0.15
−0.20
−0.1 0.0 0.1 0.2 0.3 0.4 0.5 0.6 0.7 0.8 0.9 1.0 1.1
X−AXIS
Cp

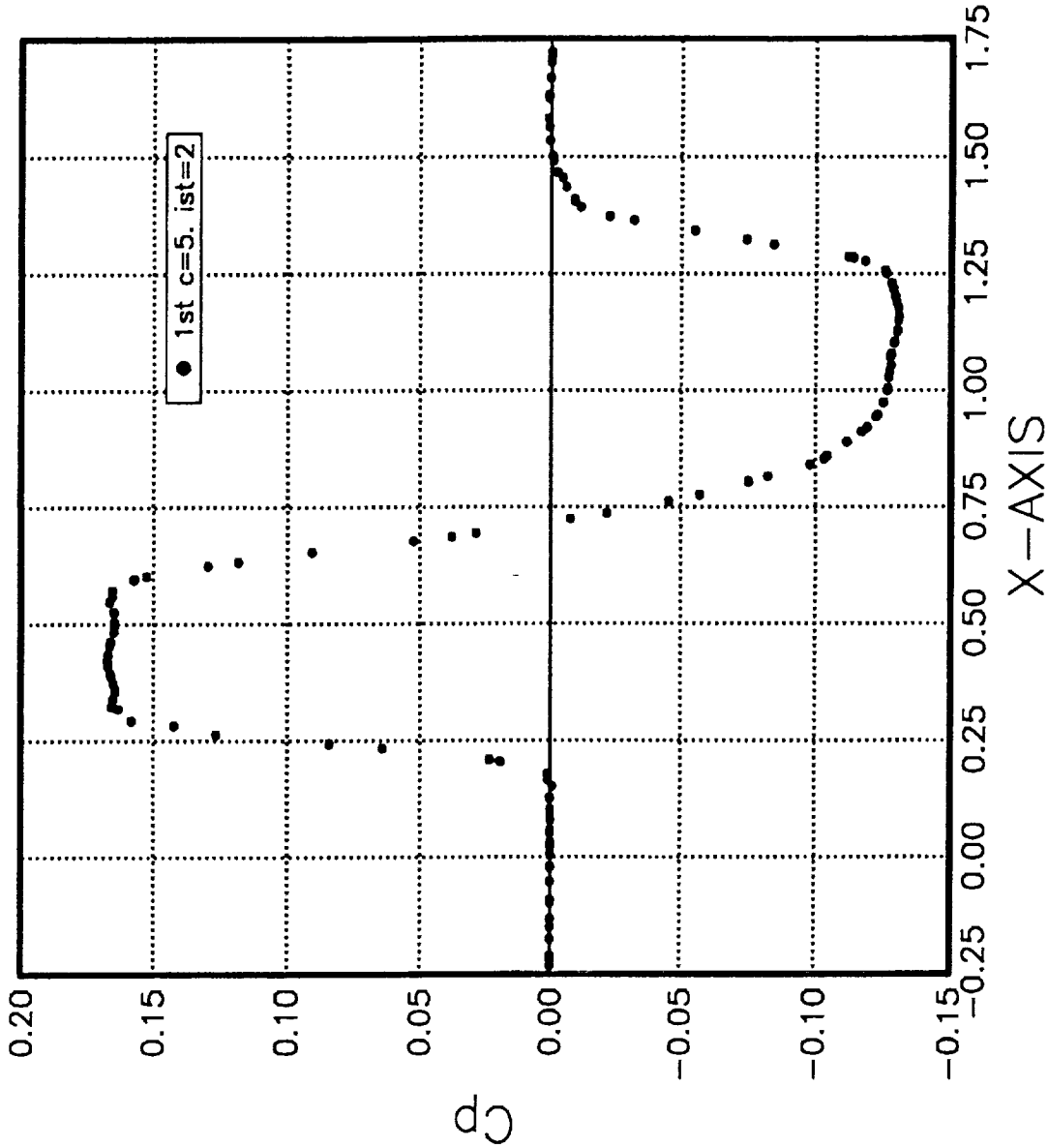
1st c=5. ist=2
0.20
0.15
0.10
0.05
0.00
−0.05
−0.10
−0.15
−0.25
0.00
0.25
0.50
0.75
1.00
1.25
1.50
1.75
Cp
X−AXIS

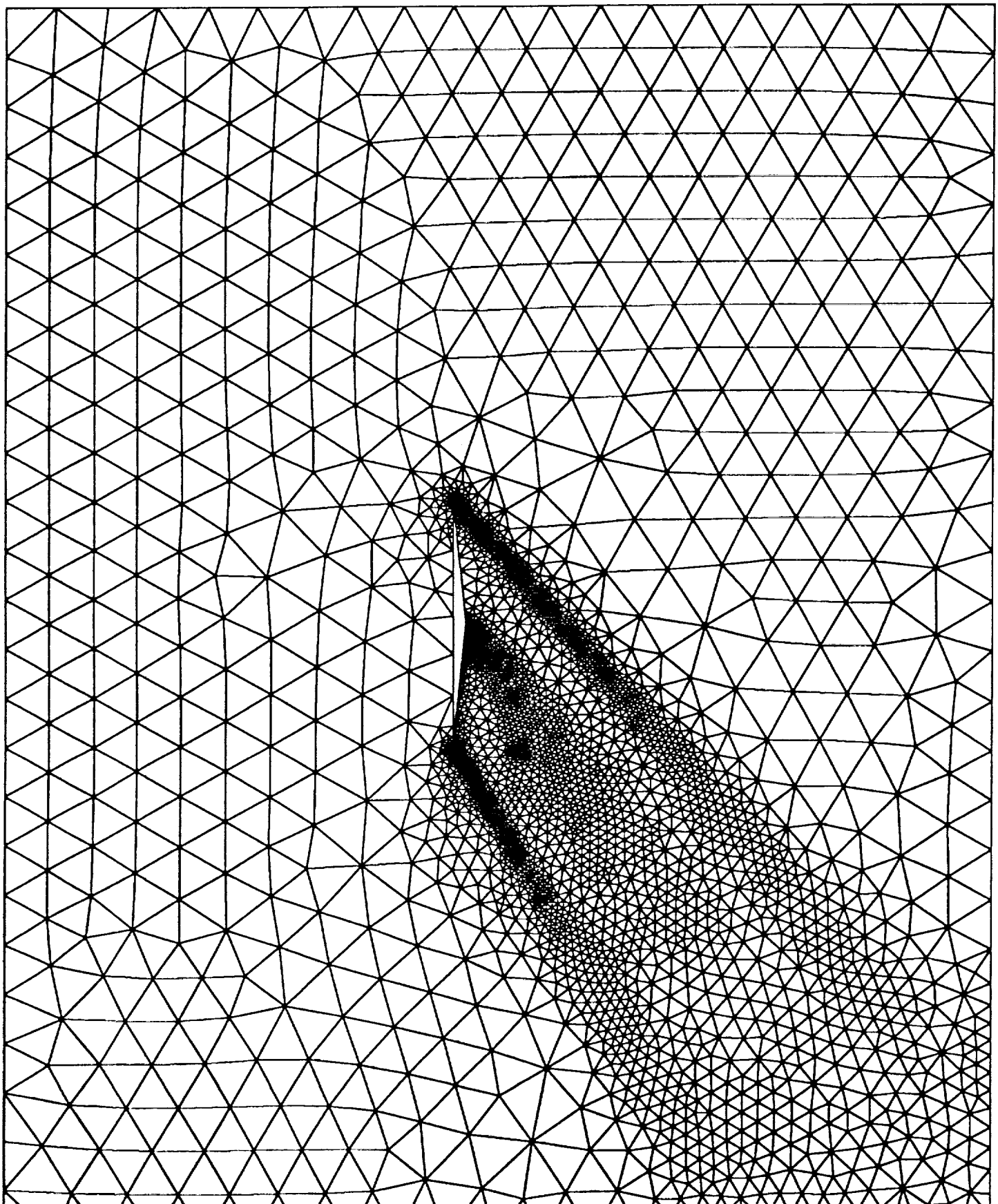

```
************************************************
 double wedge  M=1.75, a=0 -> second mesh  ***
************************************************
ber of dimensions

ements  points  boundary faces
742    15444    13654
ma  pres.sw.coef. smoothing type  epsilon ivisc     wbr
 4     5.0           2             0.       0     1.
 of far field b.c.

nf   uxinf      uyinf       uzinf       pinf       machinf
       1.        0.0         0.0       0.2332361    1.75
 of engine b.c.

me  niter  ilots(0=GLOBAL)
00     1       1
ety f. ifct nquan ido   max clima
       0   2   1 3      0.8
rmat:  g.input  u. input u.output niout
         -1       -2        1     0
oo nsmoo
  0.25   2
alpy damping coefficent
 0
dual  out  log  lift  out  log   axis    chord
        1    1          1    1    0. 0. 1.  1.
 iterations between smoothing
  1
ron  icheck
      0
ial time and iter. n.
 0   0
ut file name  (DN= )
2
2.geo

f cpu
```

21

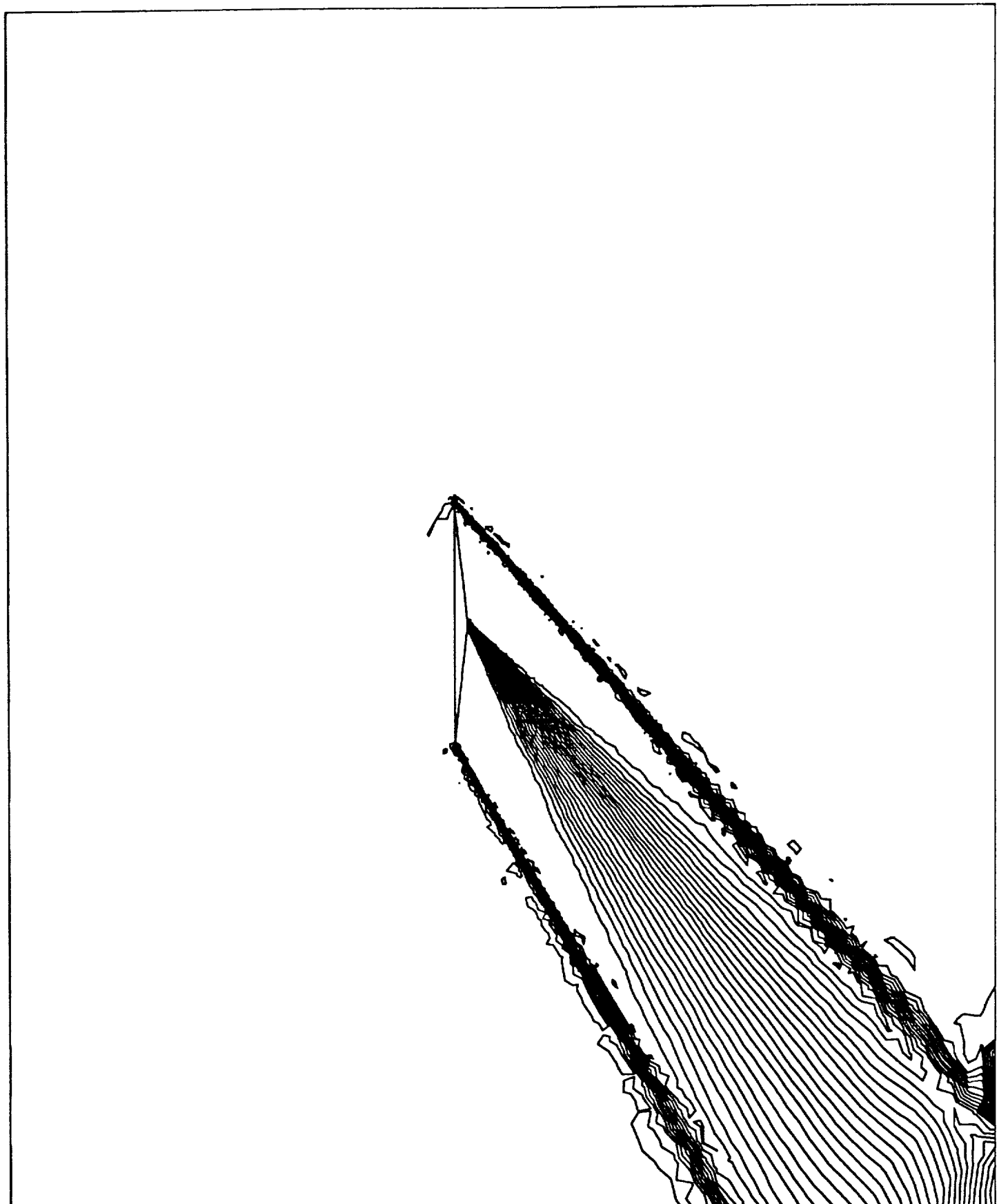

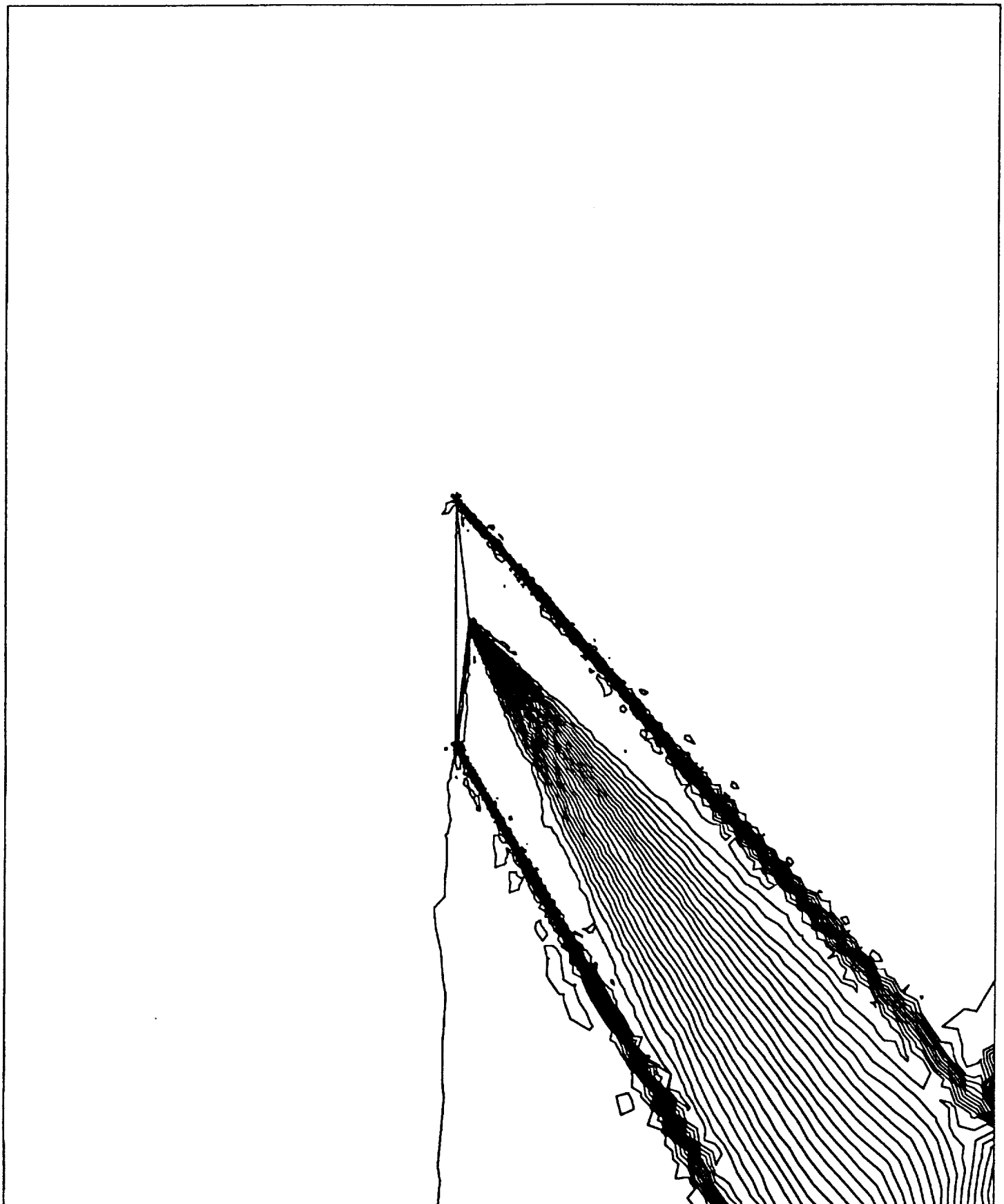

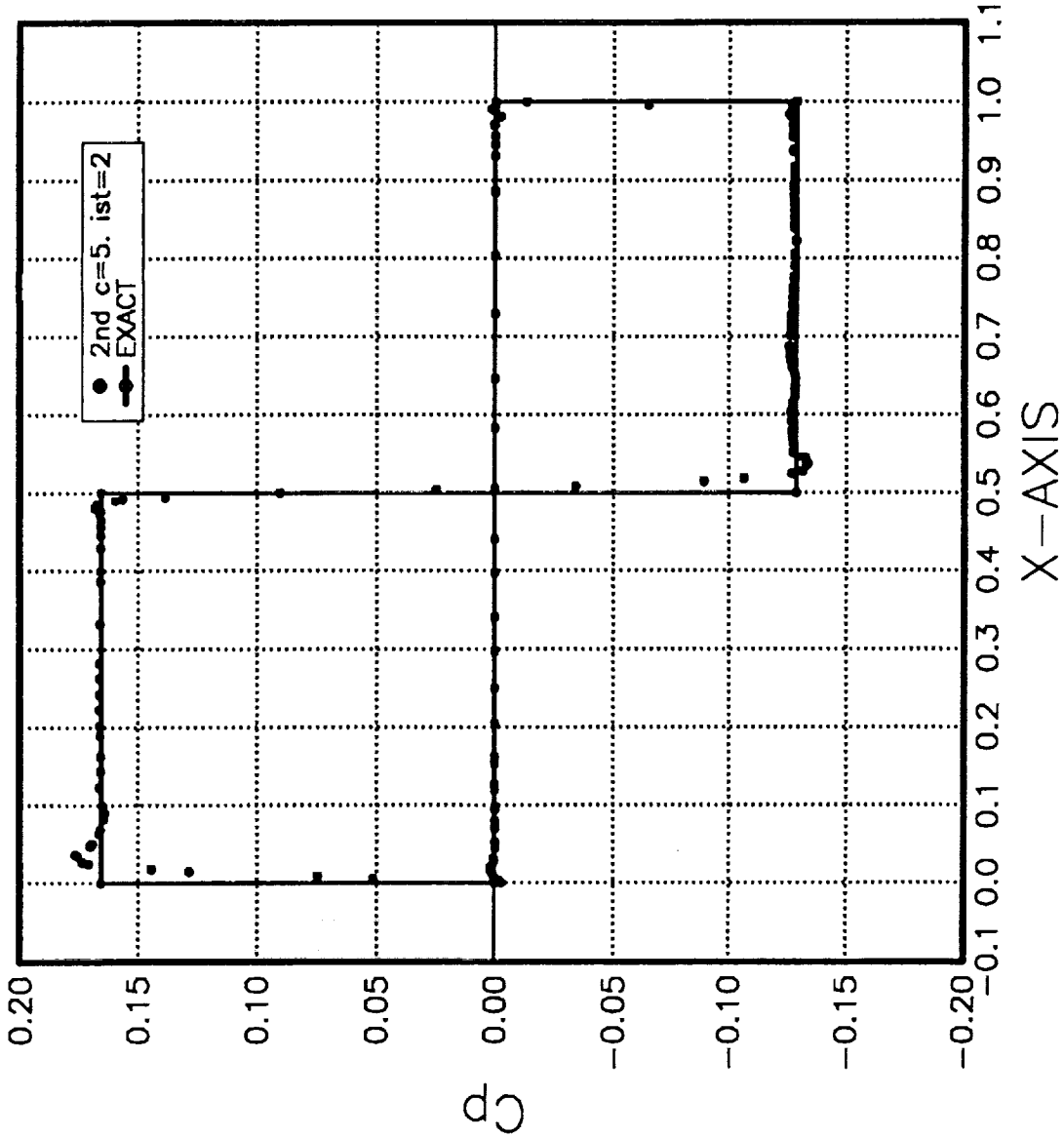
2nd c=5. ist=2
EXACT
0.20
0.15
0.10
0.05
0.00
−0.05
−0.10
−0.15
−0.20
Cp
−0.1 0.0 0.1 0.2 0.3 0.4 0.5 0.6 0.7 0.8 0.9 1.0 1.1
X−AXIS

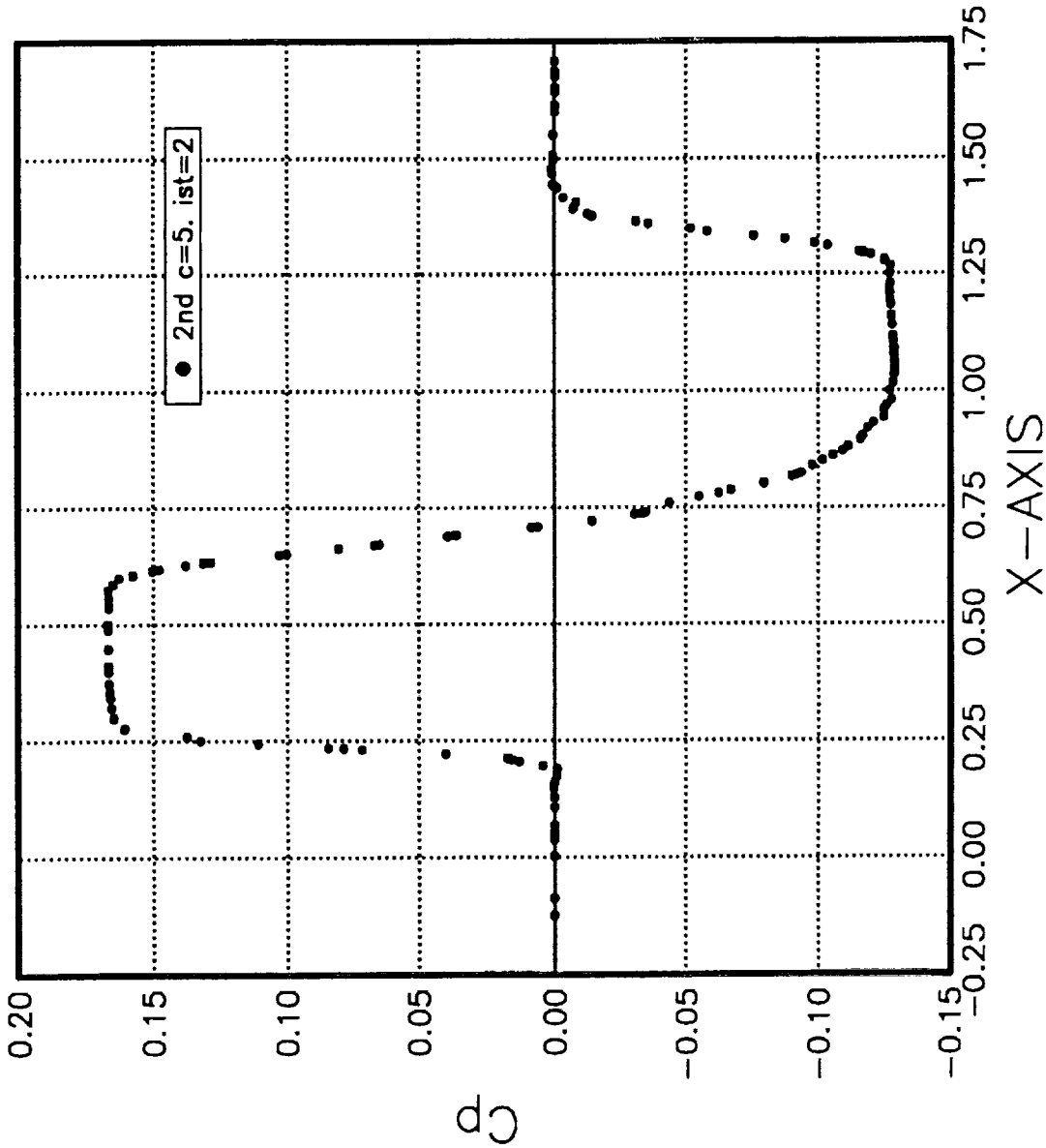
2nd c=5. ist=2
0.20
0.15
0.10
0.05
0.00
−0.05
−0.10
−0.15
−0.25
0.00
0.25
0.50
0.75
1.00
1.25
1.50
1.75
Cp
X−AXIS

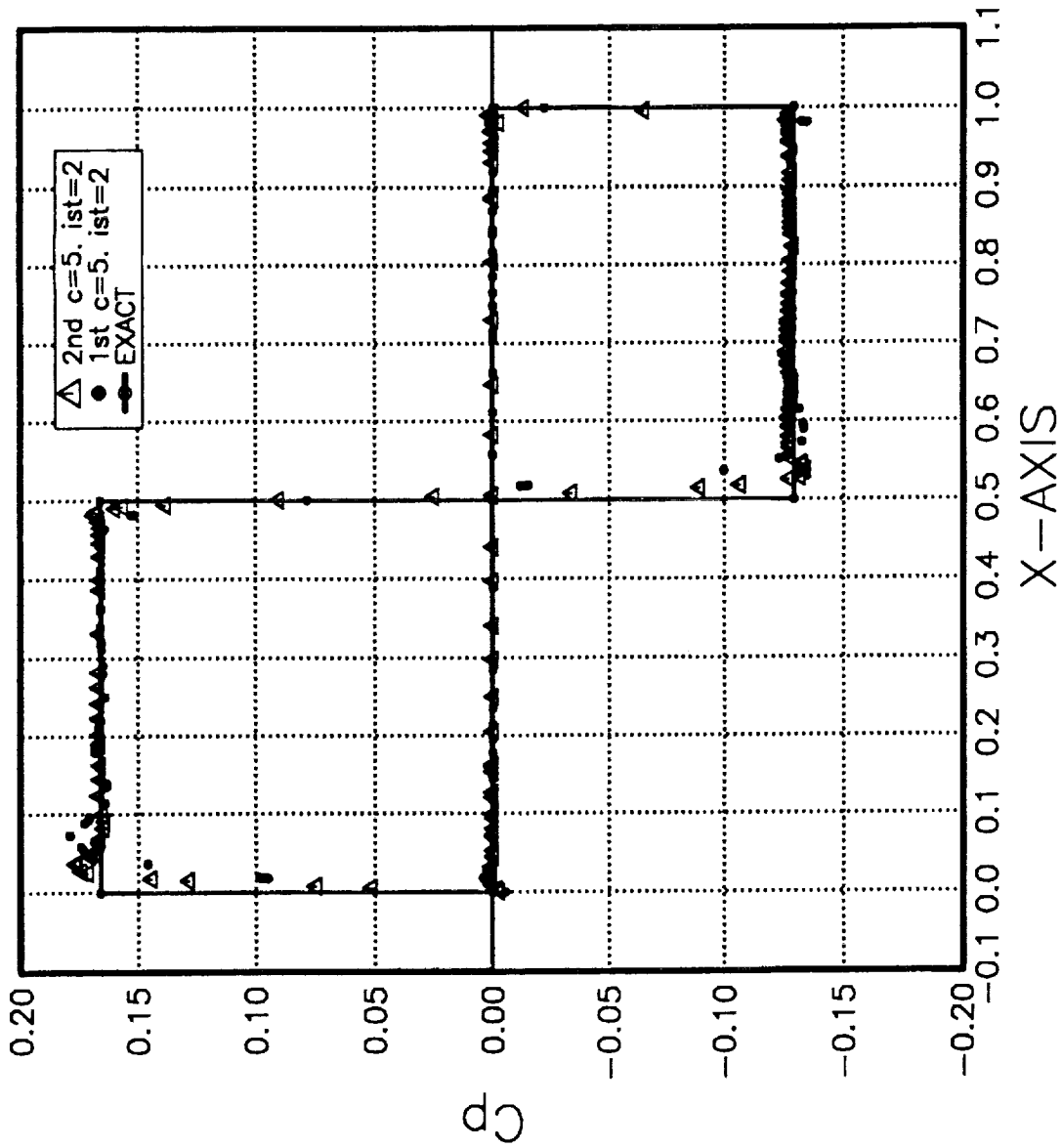
2nd c=5. ist=2
1st c=5. ist=2
EXACT
0.20
0.15
0.10
0.05
0.00
−0.05
−0.10
−0.15
−0.20
−0.1 0.0 0.1 0.2 0.3 0.4 0.5 0.6 0.7 0.8 0.9 1.0 1.1
X−AXIS
Cp

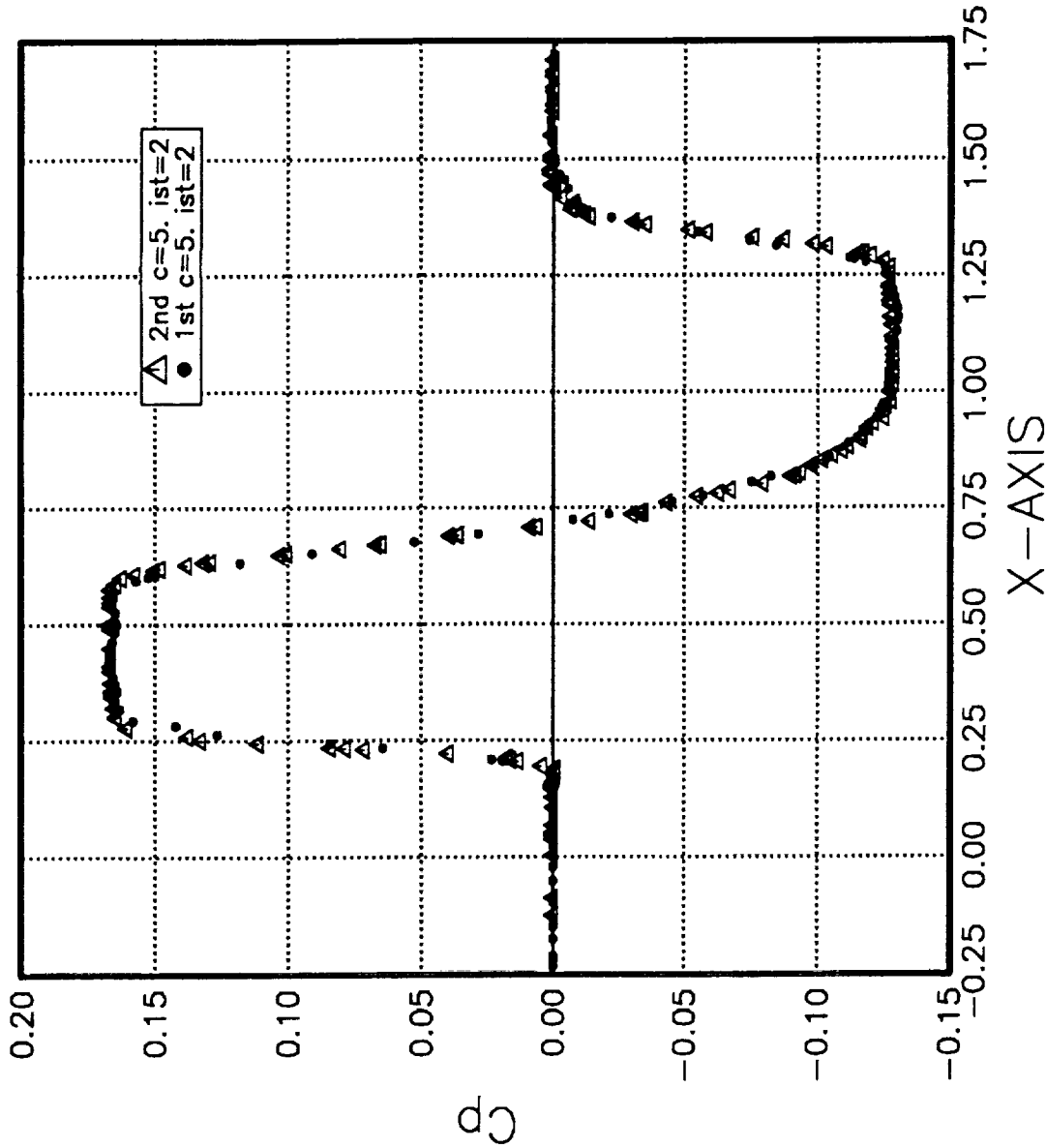
△ 2nd c=5. ist=2
● 1st c=5. ist=2
Cp
X-AXIS
0.20
0.15
0.10
0.05
0.00
−0.05
−0.10
−0.15
−0.25
0.00
0.25
0.50
0.75
1.00
1.25
1.50
1.75

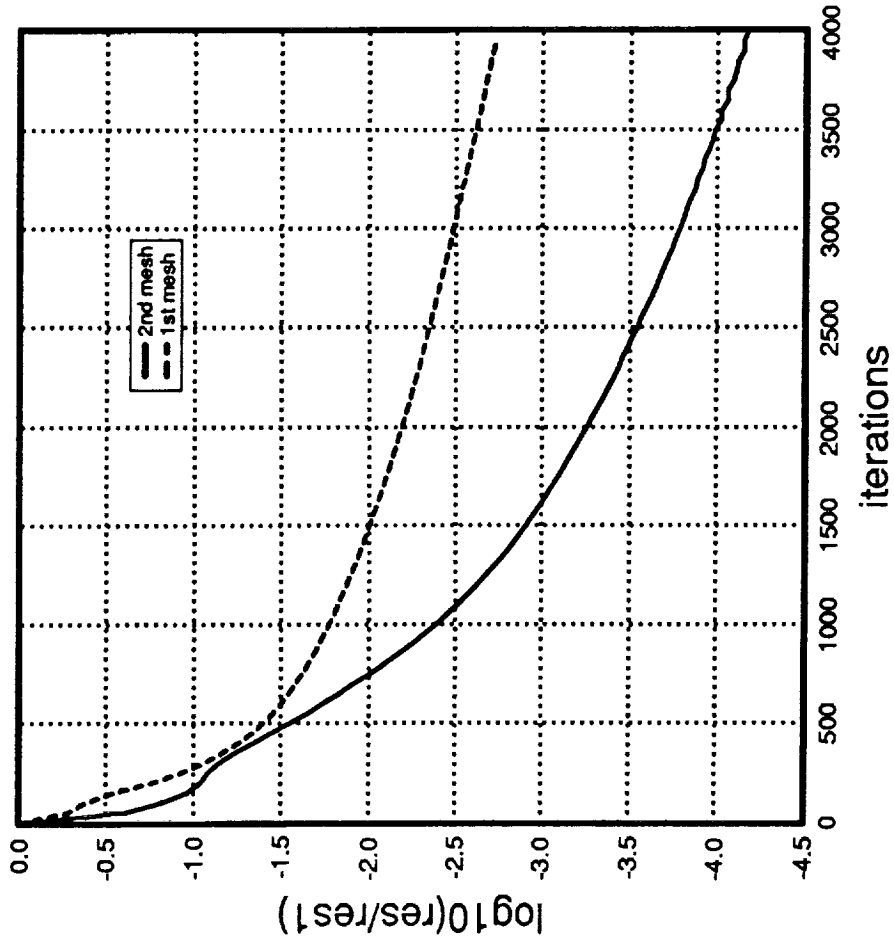
2nd mesh
1st mesh
log10(res/res1)
iterations
0.0
-0.5
-1.0
-1.5
-2.0
-2.5
-3.0
-3.5
-4.0
-4.5
0
500
1000
1500
2000
2500
3000
3500
4000

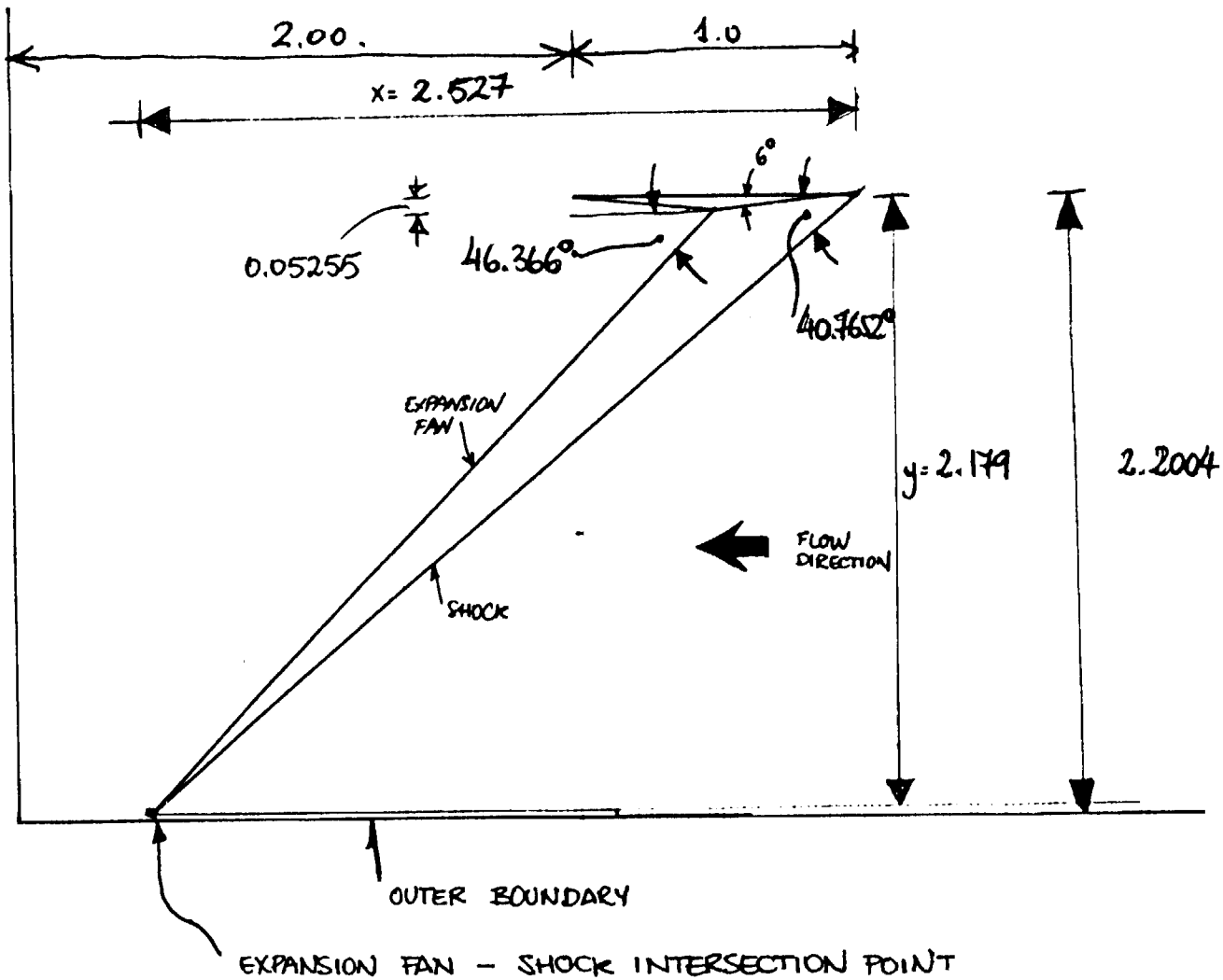

$$\frac{y}{x} = \lg 40.7652$$

$$\frac{y - 0.05255}{x - 0.5} = \lg 46.366$$

$$\Rightarrow \begin{cases} x = 2.527 \\ y = 2.179 \end{cases}$$